Bioorganic Chemistry 104 (2020) 104276

Contents lists available at ScienceDirect

Bioorganic Chemistry

journal homepage: www.elsevier.com/locate/bioorg

Design and synthesis of novel 4-thiazolidinone derivatives with promising anti-breast cancer activity: Synthesis, characterization, *in vitro* and *in vivo* results

Raheleh Tahmasvand[a,b], Peyman Bayat[c], Seyyed Mahmood Vahdaniparast[c], Soudeh Dehghani[b], Zahra Kooshafar[b], Sepideh Khaleghi[a], Ali Almasirad[c,*], Mona Salimi[b,*]

[a] Department of Medical Biotechnology, Faculty of Advanced Science and Technology, Tehran Medical Sciences, Islamic Azad University, Tehran, Iran
[b] Department of Physiology and Pharmacology, Pasteur Institute of Iran, Tehran, Iran
[c] Department of Medicinal Chemistry, Faculty of Pharmacy, Tehran Medical Sciences, Islamic Azad University, Tehran, Iran

ARTICLE INFO

Keywords:
TNBC
Thiazolidinone
Apoptosis
Metastasis
BALB/c

ABSTRACT

Novel lead compounds as anticancer agents with the ability to circumvent emerging drug resistance have recently gained a great deal of interest. Thiazolidinones are among such compounds with well-established biological activity in the field of oncology. Here, we designed, synthesized and characterized a series of thiazolidinone structures (**8a-8k**). The results of anti-proliferative assay led to the discovery of compound **8j** with a high potent cytotoxic effect using colon, liver and breast cancer cells. Furthermore, MDA-MB-231 and 4T1 cell lines were used to represent triple negative breast cancer (TNBC). Next, a number of *in vitro* and *in vivo* evaluations were carried out to demonstrate the potential activity against TNBC and also elucidate the possible mechanism of cell death induction. Our *in vitro* outcomes exhibited an impressive anticancer activity for compound **8j** toward MDA-MB-231 cells through inducing apoptosis and a remarkable anti-metastatic feature via suppressing MMP-9 expression as well. Consistently, the *in vivo* and immunohistopathologic evaluations demonstrated that this compound significantly inhibited the 4T1 induced tumor growth and its metastasis to the lung. Altogether, among numerous thiazolidinone derivatives, compound **8j** might represent a promising anticancer agent for TNBC, which is a major concern in the developed and developing countries.

1. Introduction

According to the statistics reported by WHO in Feb 2017, breast cancer ranks fifth among top causes of mortality due to cancer, which is growing both in the developed and the developing countries. Among different types of breast cancer, 266,120 new cases were diagnosed as the invasive subtypes (triple negative breast cancer, TNBC) in women in 2018 [1]. In this subtype of breast cancer, mortality frequently results from spreading of the tumor to other organs, named metastasis [2]. Treatment of the invasive breast cancer is also quite challenging because of its aggressive features [3,4]. A plentiful body of evidence revealed that promising outcome will be achieved, if the metastasis to the distant regions is prohibited [5,6]. This concern highlights an imperative need for novel therapies and causes that a great deal of attention has been drawn towards the synthesis of novel anticancer compounds capable of inhibiting metastasis.

Apoptosis is a programmed cell death which plays a decisive role in the physiological process [7]. Apoptosis is a subject that has been extensively studied among biologists and its understanding is crucial in disease condition so as it both gives information about pathogenesis and leaves clues on treatment of a disease. Cancer cells receive no signal of apoptosis due to the imbalance between cell division and cell death leading to the uncontrolled cell growth [8]. Besides, failure in apoptosis renders the tumor cells resistant to metastasis-associated death by

Abbreviations: DMEM, Dulbecco's minimum essential medium; DMSO, Dimethyl sulfoxide; ECL, Enhanced chemiluminescence; FBS, Fetal bovine serum; GAPDH, Glyceraldehyde phosphate dehydrogenase; H&E, Hematoxylin and eosin; HRP/DAB, Horseradish peroxidase/3,3'-diaminobenzidine; IC_{50}, half maximal inhibitory concentration; IHC, Immunohistochemistry; MTT, (3-(4,5-dimethylthiazol-2-yl)-2,5-diphenyl tetrazolium bromide; MMP-9, Matrix metalloproteinase-9; MVD, Microvessel density; NCBI, National cell bank of Pasteur Institute of Iran; PBS, Phosphate buffered saline; PFA, Paraformaldehyde; PI, Propidium iodide; PPAR-γ, Peroxisome proliferator-activated receptor gamma; PS, Phosphatidyl serine; PVDF, Polyvinylidene difluoride; SDS-PAGE, Sodium dodecyl sulfate polyacrylamide gel electrophoresis; SI, Selectivity index; TNBC, Triple negative breast cancer

* Corresponding authors.
E-mail addresses: almasirad.a@iaups.ac.ir (A. Almasirad), salimimona@pasteur.ac.ir (M. Salimi).

https://doi.org/10.1016/j.bioorg.2020.104276
Received 22 June 2020; Received in revised form 8 August 2020; Accepted 9 September 2020
Available online 12 September 2020
0045-2068/

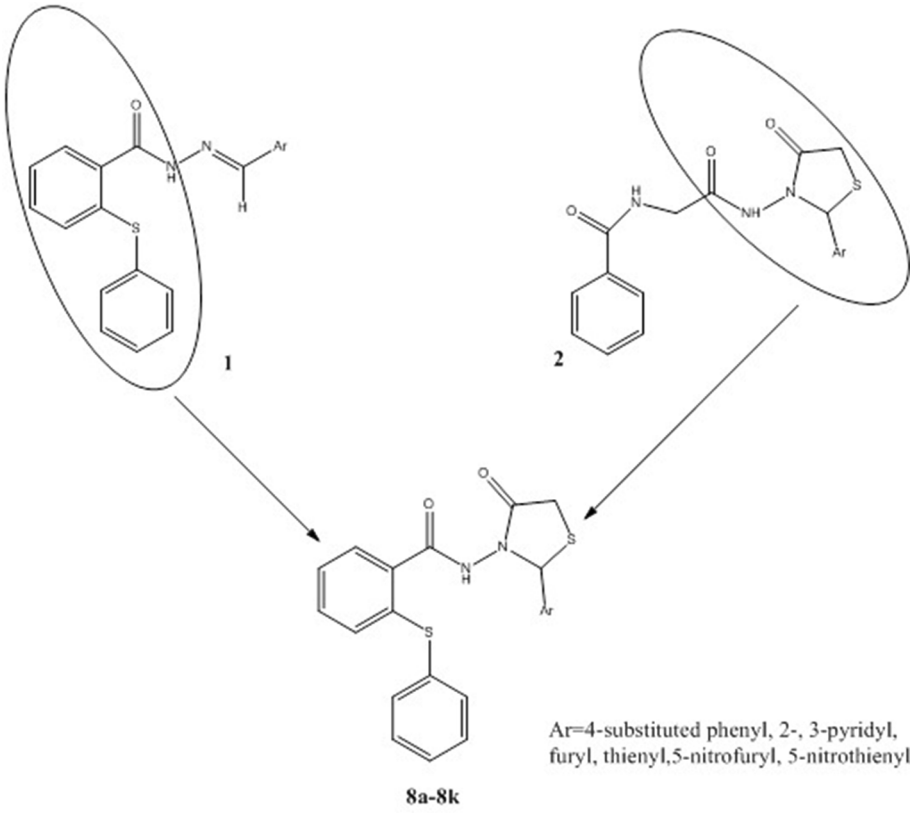

Scheme 1. Structural design of compounds **(8a-8k).**

enhancing tumor progression [9]. In this regard, compelling evidence indicated that inducing apoptosis is one of the mechanisms by which the chemotherapeutic agents act. Moreover, many of toxic side effects induced by chemotherapeutics have roots in sensitivity of the normal cells to apoptosis [10]. Therefore, continuing interest over the years has been allocated to design chemical derivatives that their underlying mechanism would be apoptosis induction in order to fight cancer cells with nominal side effects on normal cells.

Among chemical derivatives, thiazolidinone as a privileged structure has been well recognized in medicinal chemistry owing to its diverse biological activity including anticancer [11]. Several reports have revealed that thiazolidinones induce apoptosis through activating PPAR-γ [12,13]. Interestingly, researchers from time to time modified the thiazolidinone scaffold to potentiate its efficacy and lessen the related toxicity [14]. On the other hand, in our previous studies, we reported the synthesis of new hydrazone compounds possessing diphenyl thioether moiety (compound **1** in Scheme 1) with noteworthy anticancer activity [15,16]. Keeping in mind these data along with knowing that thiazolidinone is an important anti-cancer pharmacophore (compound **2**, scheme 1) [17], herein, new hybrid molecules bearing diphenyl thioether ring and thiazolidinone heterocycle were designed with aim of exploring novel and potential chemical entities useful in treatment of invasive triple negative breast cancer via inducing apoptosis (compounds **8a-8k)** (Scheme 1). The substituted phenyl and their bioisosteric replacements were selected as the first major factor in designing the thiazolidinone compounds. In order to evaluate whether the phenyl group plays an essential role in anticancer activity, we replaced the phenyl group with its bioisosteres; thienyl, furyl and pyridyl at different positions. Moreover, a diverse of the substituted phenyl derivatives containing electron withdrawing as well as electron donating groups at the *para* position of the phenyl were designed. Besides it and based on our previous experience indicating the potential role of nitro substitution in inhibiting the growth of cancer cells, we also introduced a nitro moiety in the thienyl and furyl rings [15,16].

2. Results

2.1. Chemistry

A diverse array of derivatives **(8a-8k)** were synthesized according to Scheme 2 and then characterized by physical and spectral data (IR, ^{1}HNMR, ^{13}CNMR, Mass). The hydrazide **7** was prepared as described in our previous study, starting by dissolving the thiosalicylic acid and bromobenzene in DMF, adding $NaHCO_3$ plus Cu powder and refluxing the mixture for 7 h to give compound **5** [18–20]. Compound **6** was synthesized by esterification of compound **5** with methanol in the presence of sulfuric acid and then boiling the solution for 24 h. The treatment of hydrazine hydrate at room temperature with **6** in ethanol for about 8 h was applied to synthesize **7** as the key intermediate. The hydrazide **7** and corresponding aromatic aldehydes were refluxed in toluene and then thioglycolic acid was added and refluxed again to give compounds **8a-8k.**

2.2. Compound *8j* inhibited breast cancer cell growth in vitro

3-(4,5-dimethylthiazol-2-yl)-2,5-diphenyltetrazolium bromide (MTT) assay is an usual approach in anti-cancer drug evaluation and considered as a primary screening test to determine cytotoxicity of the potential medicinal agents. To do it, the percentage of cell cytotoxicity of the thiazolidinone derivatives **(8a-8k)** was determined against MDA-MB-231, HT-29 and HepG2 cell lines at 72 h (Table 1). For N-(2-(5-nitrofuran-2-yl)-4-oxothiazolidin-3-yl)-2-(phenylthio) benzamide **(8j)** inducing a cytotoxicity more than 60%, quantification of its ability to inhibit the cell growth was performed by determining the IC_{50} value against a panel of cancer cells (MDA-MB-231, HepG2 and HT-29) to ensure its cytotoxic impact after 24, 48 and 72 h of incubation. As the results shown in Table 2, compound **8j** exhibited a time and concentration-dependent cytotoxic activity towards different cancer cell lines; however, MDA-MB-231 cells as an *in vitro* model of TNBC was our

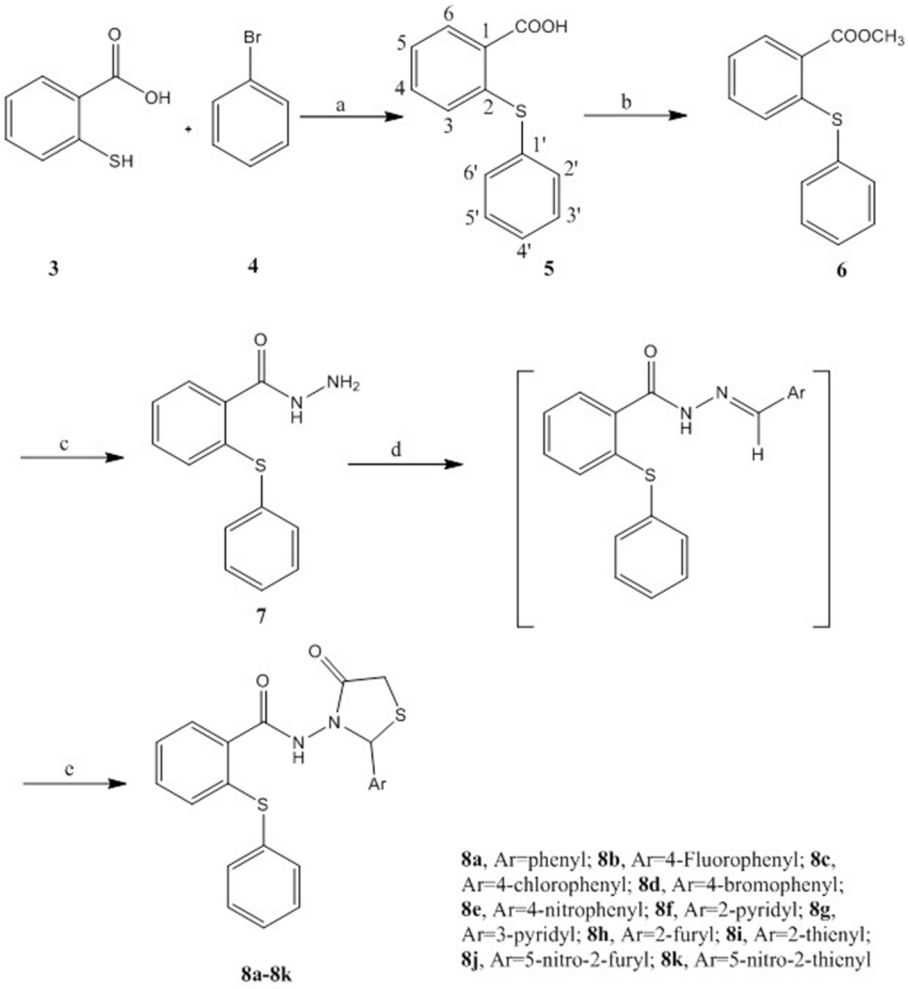

Scheme 2. Synthesis of compounds (**8a-8k**). Reagents and experimental conditions were as follows: (a) Na2CO3, Cu powder, DMF, reflux, 7 h; (b) H2SO4, CH3OH, Reflux, 24 h; (c) Hydrazine hydrate, EtOH, Stir, 8 h; (d) ArCHO, toluene, reflux, 3 h; (e) Thioglycolic acid, ZnCl2, toluene, reflux, 24–48 h.

Table 1
Cytotoxicity screening for compounds **8a-8k** following treatment at 10 μM for 72 h, towards human cancer cell lines.[a.]

Compounds	Cytotoxocity (% of Control/Vehicle)		
	MDA-MB-231	HepG2	HT-29
8a	34.92 ± 4.37	24.66 ± 1.00	ND
8b	38.48 ± 3.13	11.07 ± 2.76	5.5 ± 2.23
8c	43.08 ± 7.04	7.37 ± 1.38	4.89 ± 1.39
8d	35.92 ± 4.86	29.84 ± 1.66	9.15 ± 2.34
8e	24.76 ± 8.46	15.16 ± 0.98	4.52 ± 1.46
8f	10.33 ± 0.81	18.53 ± 2.73	6.58 ± 1.59
8g	13.06 ± 1.04	23.31 ± 2.11	2.18 ± 0.5
8h	6.1 ± 2.38	16.13 ± 1.85	ND
8i	16.53 ± 5.19	11.37 ± 1.88	ND
8j	93.02 ± 0.94	91.44 ± 0.35	74.29 ± 0.54
8k	28.74 ± 5.98	9.22 ± 3.25	2.09 ± 0.87
Control/Vehicle	3.1 ± 1.14	2.71 ± 5.2	2.71 ± 0.7
Doxorubicin	95.96 ± 0.23	90.16 ± 0.7	74.74 ± 0.58

[a] Values were determined at least three independent experiments each performed in triplicate and expressed as mean ± SEM. ND: Not Determined.

ultimate goal. Given the results, compound **8j** with the IC_{50} value of 1.9 μM revealed a high potential in cell growth inhibition of MDA-MB-231 cells at 72 h. Interestingly, this compound exerted a certain extent viability toward the normal cell line, HGF-1 (IC_{50} = 13.5 μM) at 72 h (Table 2). Moreover, selectivity index (SI) manifested a selection of compound **8j** activity between normal fibroblastic cell and cancer cell (SI greater than 7).

Table 2
IC_{50} values for cytotoxic activity of compound **8j** towards human cancer cell lines.[a.]

	IC_{50} (μM)		
Cell lines/time	24 h	48 h	72 h
MDA-MB-231	58.84 ± 1.13	4.1 ± 1.08	1.9 ± 1.15
HepG2	7.0 ± 1.08	7.1 ± 1.08	5.4 ± 1.13
HT-29	16.37 ± 1.17	10.9 ± 1.13	6.5 ± 1.16
HGF-1	—	—	13.51 ± 1.12

[a] Values were determined at least three independent experiments each performed in triplicate and expressed as mean ± SEM.

2.3. Compound *8j* induced cell apoptosis

Apoptosis induced by compound **8j** in tumor cells was quantitatively determined by flow cytometry. Phosphatidylserine (PS) in the inside of the cell membrane is translocated to the outside in the early stages of apoptosis and forms a complex with annexin V. Thus, annexin V fluorescence is directly proportional to the population of apoptotic cells, while PI stains the cells undergoing necrotic changes. Cells stained with Annexin V-FLUOS and PI are distinguished as necrotic cells (Q1, annexin-/PI +), late apoptotic cells (Q2, annexin+/PI +), intact cells

Table 3
Percentage of MDA-MB-231 cells in each state after treatment with compound **8j** at 48 h.[a]

Concentration	Vital cells (%)An-/PI-	Early apoptosis (%) An+/PI-	Late apoptosis (%) An+/PI+	Necrosis (%)An-/PI+
2 μM	96.33 ± 0.33	1.05 ± 0.30	0.58 ± 0.023	1.7 ± 0.09
4 μM	94.23 ± 0.40**	2.25 ± 0.31*	0.7 ± 0.044	2.8 ± 0.23**
8 μM	79.7 ± 1.04****	3.4 ± 0.085**	2.48 ± 0.37***	13.46 ± 0.3****
Control/vehicle	98.46 ± 0.10	0.82 ± 0.14	0.33 ± 0.024	1.03 ± 0.02

[a] The data presented are the mean ± SEM of three independent experiments. *$p < 0.05$, **$p < 0.01$, ***$p < 0.001$, ****$P < 0.0001$ compared with control.

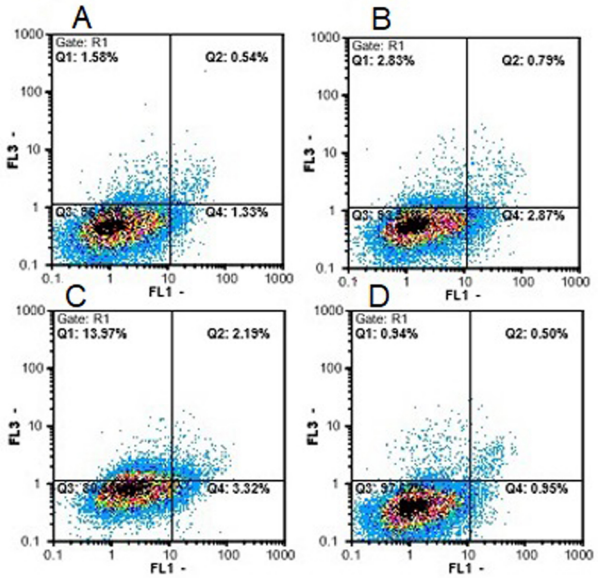

Fig. 1. Annexin-V/PI flowcytometric analysis to quantify compound **8j**-induced apoptosis in MDA-MB-231 cells. Dot plot of MDA-MB-231 cells treated with compound **8j** at (A) 2 μM (B) 4 μM (C) 8 μM (D) Control/Vehicle for 48 h. The results shown are representatives of three independent experiments. Quadrant 3, living cells An−/PI−; Quadrant 4, early apoptotic cells An+/PI−; Quadrant 2, late apoptotic cells An+/PI+; Quadrant 1, necrotic cells An−/PI+.

(Q3, annexin-/PI-) and early apoptotic cells (Q4, annexin +/PI-). As illustrated in Table 3, 2 μM concentration of compound **8j** caused no apoptosis induction in MDA-MB-231 cells after 48 h of treatment. However, cell population at the early and late stages of apoptosis increased gradually in a concentration-dependent manner following treatment of MDA-MB-231 cells with 4 and 8 μM concentrations. As depicted in Table 3, the percentage of early apoptotic cells increased from 0.82% in the untreated cells to 2.25% and 3.4% in the cells treated with 4 and 8 μM of compound **8j**, respectively, at 48 h. Furthermore, apoptotic cell percentages in the late stage were 0.7% at 4 μM and 2.48% at 8 μM concentrations vs. 0.33% for the control cells. A significant increased number of annexin V positive cells were visualized following compound **8j** treatment at 4 μM compared with the control cells (Fig. 1). Due to the highest rate of necrosis upon treating with the 8 μM, we excluded it and focused our further experiments on the other two concentrations.

One of the features in process of apoptosis is morphologic changes [21]. In this regard, DAPI staining displays the nuclei possessing cytopathic marks typical of apoptosis including DNA condensation and fragmentation into apoptotic bodies. To find out whether compound **8j** caused nuclear shrinkage and DNA fragmentation, MDA-MB-231 cells were incubated with 2 and 4 μM concentrations for 48 h, and then stained with DAPI (Fig. 2). In the control, the living cells presented homogeneous nuclei staining in spots. The nucleus of the 4 μM -treated cells demonstrated a condensed blue-fluorescence with the fragmented apoptotic bodies.

Caspases are believed to execute apoptosis through processing of their substrates, which leads to the morphological changes associated with apoptosis including membrane blebbing, DNA degradation and chromatin condensation [22]. Hence, caspase-3 activity was determined following treatment of MDA-MB-231 cells with 2 and 4 μM concentrations of compound **8j** at 48 h. Since the caspase-3 antibody applied for our Western blotting analysis could not well detect the active 17-kDa subunit, the activation/processing of caspase-3 was assessed by cleavage of the 32-kDa precursor form. As shown in Fig. 3, after treatment with 4 μM concentration of compound **8j**, the expression level of pro caspase-3 decreased compared to that in the control cells, whereas no obvious change was found following treatment with 2 μM of compound **8j**. Overall, our results indicated that compound **8j** induced apoptosis by regulating pro-caspase 3.

2.4. Evaluating the cell cycle progression following compound *8j* treatment

To further explore whether the anticancer activity of compound **8j** is via cell cycle arrest, we analyzed the treated and non-treated MDA-MB-231 cells after 48 h. MDA-MB-231 cells treated with compound **8j** at different concentrations, 2 and 4 μM, exhibited a typical DNA pattern representing G0/G1, S, and G2/M phases of the cell cycle (Fig. 4). MDA-MB-231 cells displayed a higher G0/G1 population (73.4%) compared with 62.87% in the control when treated with 2 μM concentration of compound **8j**. The accumulation of cells in G0/G1 phase was augmented by increasing the concentration to 4 μM by 77.7%. While concomitantly the proportion of cells in S phase decreased from 33.5% in the untreated cells to 24.60% and 23.17% in the cells treated with compound **8j** at 2 and 4 μM concentrations, respectively. Similarly, G2/M cells percentage decreased from 7.1% in the control cells to 5.08% and 5.1% in the treated cells. These findings indicated that cells did not enter into the S phase and corroborated that the compound **8j** affected cell cycle progression before the G1/S checkpoint. The occurrence of cell growth arrest at G1/S phase along with the increase in G0/G1 population following treatment with this compound at the two mentioned concentrations further explored the apoptotic effect of compound **8j** in the breast cancer cells.

2.5. Compound *8j* promoted anchorage-independent growth

In order to verify the inhibitory effect of compound **8j** on the anchorage-independent growth and self-renew of breast cancer cells, soft agar colony formation assay as a hallmark of cancer cells was carried out and defined as the capability of the cells to independently grow on a solid surface [23]. The results demonstrated that upon treatment of the cells with compound **8j** at 4 μM as the most effective concentration for 48 h, significantly less colonies were formed when compared to the control cells (237.3 ± 14.11 vs. 303.2 ± 7.3) (Fig. 5).

2.6. Anti-invasive property of compound *8j*

To explore the effect of compound **8j** on the metastatic feature of highly invasive TNBC cells, we performed matrigel invasion test on MDA-MB-231 cells treated with the 4 μM concentration of compound **8j** based on our apoptosis induction evaluation. We found out that

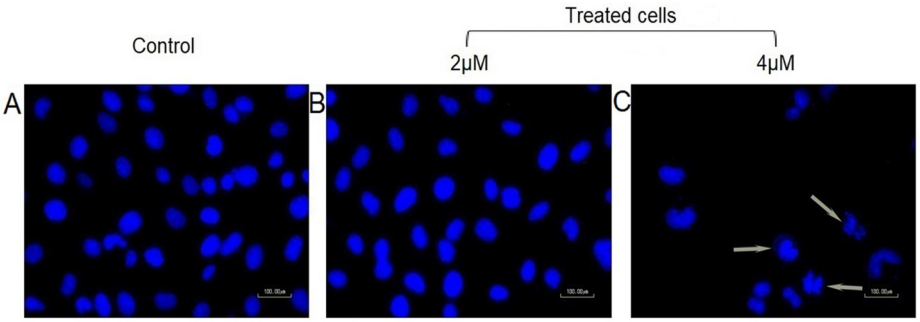

Fig. 2. Nuclear staining assay by using DAPI on human breast cancer, MDA-MB-231 cells in the presence and absence of compound **8j**. (A) Untreated and treated cells with (B) 2 μM and (C) 4 μM concentrations for 48 h. The morphological changes were observed using fluorescent microscope (20X).

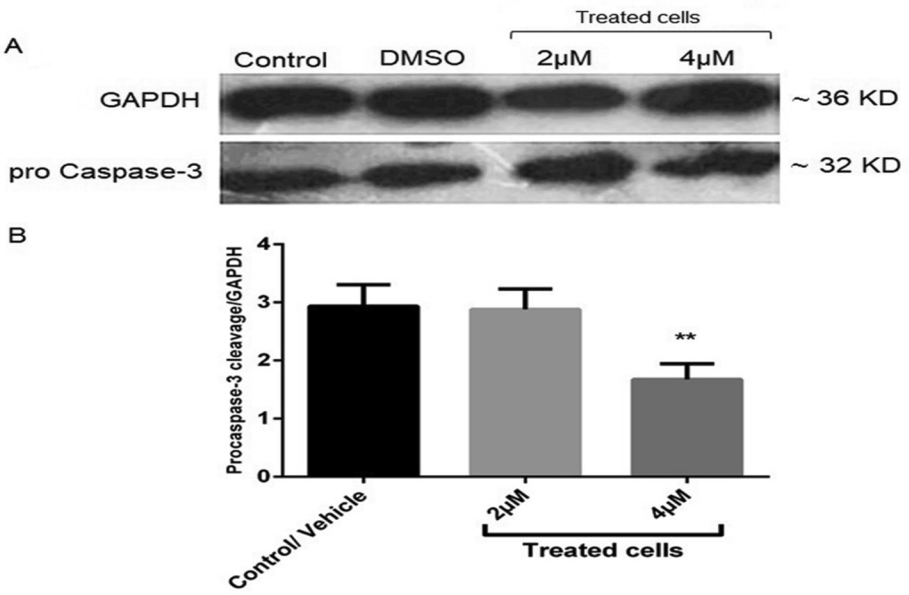

Fig. 3. Expression of procaspase-3 in MDA-MB-231 cells induced by 2 and 4 μM concentrations of compound **8j** for 48 h. GAPDH was used as internal control. (A) Relative level of procaspase-3 expression was calculated and normalized to the loading control. (B) Corresponding protein levels were assessed using densitometry. Each value represents the mean ± SEM of three independent experiments, one-way ANOVA analysis with Tukey post test was performed ($^{**}p < 0.01$ comparing to the control/vehicle cells).

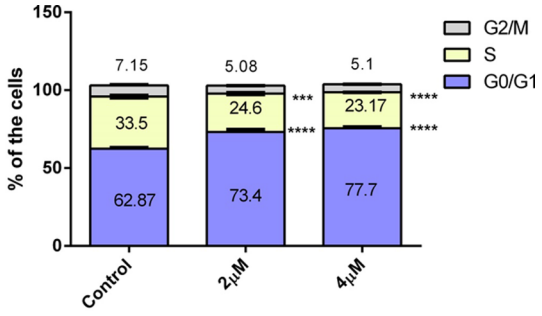

Fig. 4. Cell cycle phase distribution of MDA-MB-231 cells treated with compounds **8j** for 48 h. The data presented are the mean ± SEM of three independent experiments of MDA-MB-231 cell cycle phase. Differences in the data was compared with control using two way ANOVA ($^{***}p < 0.001$, $^{****}p < 0.0001$).

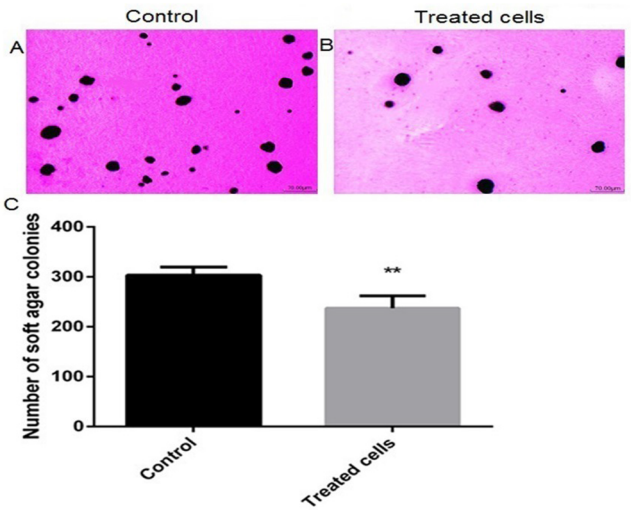

Fig. 5. Visualization of soft agar colony formation in (A) untreated and (B) treated MDA-MB-231 cells with 4 μM concentration of compound **8j** for 48 h. (C) Quantification of colonies in the assay described in (A, B) performed using Image J software of a representative experiment by unpaired *t* test, $^{**}p < 0.01$.

compound **8j** diminished the invasive ability of MDA-MB-231 cells compared to that of the control cells after 48 h of exposure (Fig. 6).

*2.7. Compound **8j** down-regulated MMP-9 mRNA expression level*

It has been reported that MMPs are closely associated with tumor growth, invasion and metastasis [24,25]. Among MMPs family, MMP-9 contributes to breast cancer metastasis [26] as well as tumor angiogenesis [27]. Thus, we aimed to ascertain that the anti-metastatic effect of compound **8j** is through down regulating the mRNA expression of MMP-9. Our findings showed that expression level of MMP-9 after treatment with compound **8j** (4 μM) was significantly diminished compared to the untreated cells (Fig. 7). Notably, MDA-MB-231 cells

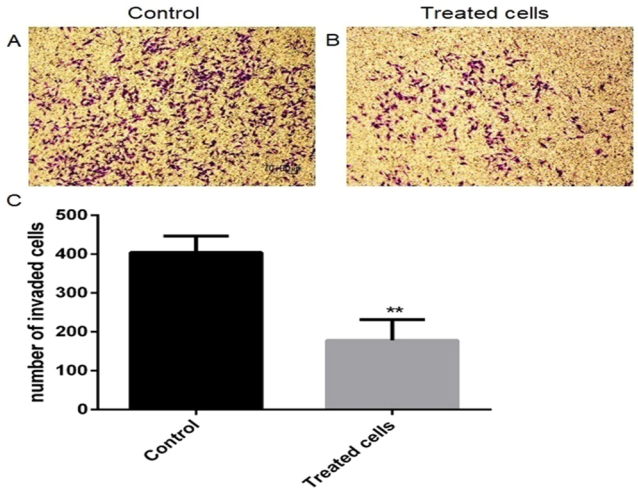

Fig. 6. Effect of compound **8j** on the invasiveness of MDA-MB-231 cells. The cells were cultured in the presence of 4 μM concentration of the compound for 48 h within a matrigel invasion chamber. (A, B) Microphotographs of filters in the untreated and treated cells and (C) Quantitative analysis of the invaded cells. Differences in the invasiveness was compared with control using unpaired *t* test ($^{**}p < 0.01$).

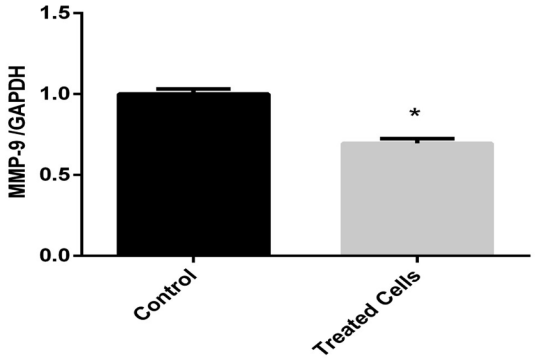

Fig. 7. MDA-MB-231 cells were incubated with compound **8j** (4 μM) for 48 h. The cells were subsequently assayed for MMP-9 mRNA expression by quantitative Real-time PCR. Results are presented as the mean ± SEM of three independent experiments. Unpaired *t* test analysis ($^{*}p < 0.05$) was carried out comparing to the MDA-MB-231cells.

revealed a basal level of MMP-9 mRNA expression.

2.8. Primary tumor growth was inhibited by compound 8j

We next applied orthotopic breast tumor model to verify the antitumor activity of compound **8j** on breast tumor growth and metastasis, since this model has been designated as a well-established prototype to mimic human breast cancer in an immune-competent situation. To create this model, 4T1 cells were inoculated into the mammary fat pad of female BALB/c mice. Compound **8j** (1 and 10 mg/kg) was intraperitoneally administered daily for 20 days, once tumor was palpable. A reduction in tumor size was dramatically observed after 2, 3 and 4 weeks of compound **8j** treatment. A 33% and 60% reduction in the tumor growth was distinguished following 1 and 10 mg/kg of compound **8j** treatment, respectively, at the termination of experiment. On the other hand, volume of the tumor in the control group increased rapidly after a 4-week investigation, while the growth of the tumors treated with 1 and 10 mg/kg of compound **8j** showed a slowly upward trend. The tumor volume values were: control group (401.6 ± 19.13 mm^3) and treated groups (272.4 ± 56.47 mm^3) and (157.5 ± 51.68 mm^3) for 1 and 10 mg/kg, respectively at the fourth week of treatment (Fig. 8). Indeed, compound **8j** dose-dependently

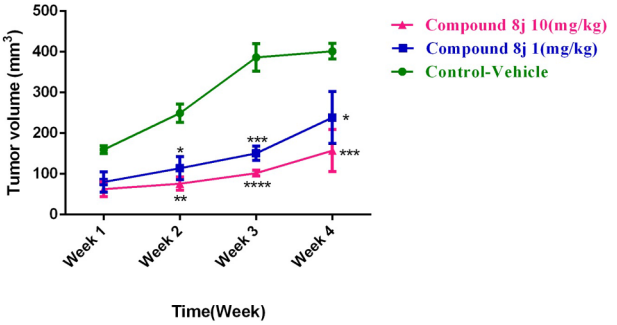

Fig. 8. Effect of compound **8j** at different doses (1 and 10 mg/kg/day) on tumor growth during the 3 weeks treatment. Data are expressed as mean ± SEM, n = 8 mice per group. Data in the treated groups was compared with the control group at each week using two way ANOVA ($^{*}p < 0.05$, $^{**}p < 0.01$, $^{***}p < 0.001$, $^{****}p < 0.0001$).

suppressed the growth of mammary tumor and 10 mg/kg of compound **8j** seems to be more effective than that of 1 mg/kg in restraining the tumor growth. Notably, no momentous body weight loss was found in the compound-treated mice during the experimental period.

The tumor sections were then subjected to histopathological analysis (H & E staining) to find out the intratumor potential of compound **8j**. The findings clearly demonstrated that the tumors treated with compound **8j** at 10 mg/kg/day underwent intratumor spaces owing to the cell necrosis; however, tumor tissues in the 1 mg/kg of compound **8j**-treated and control groups exhibited an intact structure with the large and dark-blue nucleus (Fig. 9 A, B, C). To further confirm the impact of compound **8j** on inhibition of the cell proliferation *in vivo*, immunohistochemical analysis was carried out to evaluate the expression level of a representative marker of proliferation, Ki-67 [28]. Ki-67 had a reduced expression in 10 mg/kg of compound **8j**- treated group (35%), whereas it was highly expressed in the control group (60%) (Fig. 9D, E). Since cancers that express CD-31 as an endothelial cell marker are able to spread to other organs, in the current study, tumor sections were also stained with an anti-CD31 antibody to observe microvessels. Compound **8j** at dose of 10 mg/kg/day led to a statistically significant reduction in tumor microvessel density (MVD = 31.61 ±

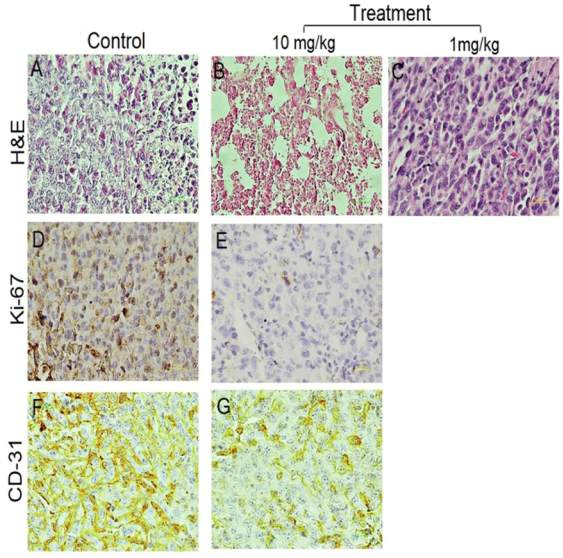

Fig. 9. Effect of daily administration of compound **8j** on solid tumors in BALB/c mice injected with 4T1 cells. The mice were killed 34 days after cell injection, and tumor sections were evaluated by (A, B, C) H&E staining and immunostaining detection of (D, E) Ki-67 and (F, G) CD 31 (original magnification ×200 and ×400).

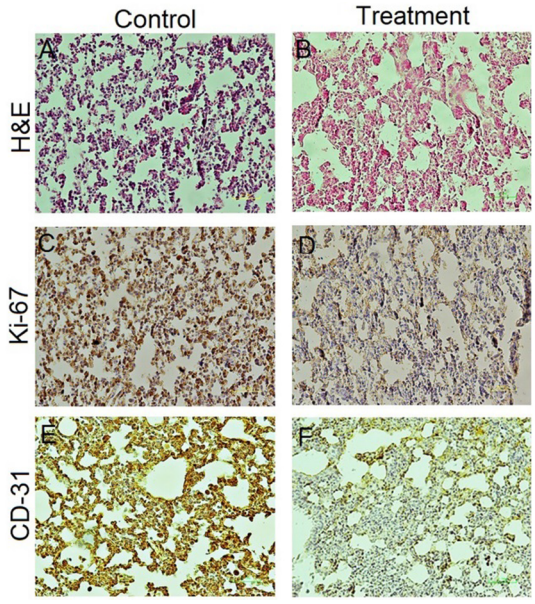

Fig. 10. Compound **8j** (10 mg/kg/day) inhibited metastasis to the lungs of BALB/c mice inoculated with 4T1 cells. (A, B) H&E staining was performed on the lungs. Upon treatment, lungs were sampled to evaluate the extent at which the cells had metastasized. Lung sections were stained with antibody raised against (C, D) Ki-67 and (E, F) CD31 and then with 1,3-diaminobenzidine (DAB) and counterstained with hematoxylin. Representative images of the immunohistochemical analysis are shown. All photomicrographs are at ×200 magnification.

3.97%) compared to the control with MVD equivalent to 53.64 ± 1.42% (Fig. 9F, G).

2.9. Compound *8j* suppressed the metastasis to lung

Given the results obtained in the matrigel and MMP-9 determination assays for compound **8j**, we next studied its anti-metastatic activity in an *in vivo* setting. To do it and to find out whether compound **8j** treatment would have therapeutic efficacy in controlling the outgrowth of metastatic tumor, the number of metastatic nodules in the lung was counted through microscopy in a 4T1 spontaneous lung metastasis model 34 days post cell injection. Our H&E results indicated that mice in the control group developed lung metastasis; however, the number of metastatic lung foci significantly decreased in the 10 mg/kg of compound **8j**-treated group (Fig. 10 A, B). Moreover, to further verify the histopathologic findings, immunohistochemistry of the lung sections were carried out using anti-Ki-67 antibody to report the proliferation index. Compound **8j** diminished the proliferation index at dose of 10 mg/kg/day compared to the control (Fig. 10C, D). The extent of pulmonary metastasis in the treated group was also assessed by determining microvessel density using anti-CD31 anti body (Fig. 10E, F). The outcomes demonstrated that compound **8j** contributed to the reduction in lung angiogenesis (39.28 ± 4.4% vs 59.8 ± 4.3% in the control lungs) corroborating its anti-metastatic property.

3. Discussion

Currently, cancer is known as a developing ecosystem in which cancer cells effectively interact with their microenvironment. The emerging drug resistance to chemotherapeutic agents used in the treatment of cancer in general and breast cancer in particular due to tumor heterogeneity has necessitated the designing of novel agents [1]. Many interesting properties were reported for compounds containing hydrazide-hydrazone moiety, among them, anti- cancer activity has been recently gained increasing attention [29]. To date, thiazolidinones with anticancer features derived from hydrazides by reacting with thioglycolic acid become a promising research area [30]. Hence, we divulged the utility of this efficient pharmacophore to design a series of compounds possessing antitumor activity **(8a-8k)**.

Structures of the synthesized compounds were confirmed by spectral analysis data. In FT-IR spectra, NH signals were found over 3100 cm^{-1} and two carbonyl groups were shown as two separate absorptions between 1664 and 1714 cm^{-1}. In proton NMR, the proton chemical shift of NH was present at 8.02–10.91 ppm. Thiazolidinone ring closure was confirmed by finding the Ar-CH as a singlet between 5.97 and 6.27 ppm and two different S-CH doublets in the range of 3.59–4.03 ppm along with a coupling constant about 16.0 Hz. In ^{13}C NMR, the two carbonyl moieties were detected from 165 to 170 ppm. The Ar-CH and S-CH peaks found near to 60.0 and 30.0 ppm, respectively. Signals at 163.35 and 161.41 ppm are related to the coupling of fluorine with C4-fluorophenyl (J = 244.4 Hz), whereas signals at 115.43 and 115.26 ppm belong to C3-, C5-fluorophenyl (J = 21.4 Hz). The coupling of fluorine with C2, C6 and C1 was not seen due to the small coupling constants. Exact mass of all the compounds were figured out by mass spectrometry. The elemental analysis results revealed the acceptable purity of the compounds.

Our preliminary study displayed that among different derivatives with thiazolidinone structure, compound **8j** bearing nitrofuran group induced a remarkable cytotoxicity on MDA-MB-231 cells as an *in vitro* model of TNBC, the most challenging subtype of breast cancer. Such cytotoxicity of the compounds is attributed to the presence of the thiazolidinone ring bearing substituted phenyl or its bioisosteres. Comparing the cytotoxic activity of compounds **8a-8k**, bioisisteric replacement of phenyl (compound **8a**) with some heteroaromatic rings (2- or 3-pyridyl-, 2-furyl- or 2-thienyl-) led to a deteriorative effect on the cytotoxic activity. Moreover, presence of halogens as non-polar electron withdrawing groups on *para* position of the phenyl ring was tolerable, although it was resulted in decreasing the activity in a way that by increasing the atomic radius and decreasing the electronegativity of halogens, the effect became weak (compounds **8b**, **8c** and **8d)**. In contrast to halogens, insertion of nitro as a polar and strong electron withdrawing group (**8e**) reduced the activity. Thus, it can be assumed that a hydrophobic pocket in the receptor is near to the *para* position of phenyl ring. Notably, substitution on the phenyl ring was not beneficial to create cytotoxic compounds. The most potent compound obtained by adding the nitro group on the 2 position of the furan ring (compound **8j**), which may be attributed to different orientation of nitro group in comparison to **8e**. The more strong cytotoxic activity of **8j** than that of its analogue **8k** may be associated with the plausible hydrogen bonding of oxygen in furan compared with sulfur in the thiophen ring. These findings are in agreement with other studies corroborating the presence of nitrofuran as an important pharmacophore in various derivatives with anticancer activity [31–34]. Hence, compound **8j** was selected for further investigation.

In the current study, we reported for the first time that compound **8j** could significantly inhibit growth of the breast cancer *in vitro* and *in vivo* with induction of apoptosis as a main mechanism of action suggesting that it could be a promising anticancer therapeutic agent. *In vitro* cytotoxicity assay exhibited that this compound could strongly kill the breast cancer cells with a low IC_{50} value (1.9 μM) after 72 h of treatment. Based on our literature survey, anti-cancer agents possessing SI value of more than 2 toward normal cell line indicate a best compromise between a strong activity and high selectivity [35]. Consistently, our findings represent a desirable selectivity along with a powerful activity for compound **8j** on a triple negative breast cancer cell line. Another feature of the cancer cells is their anchorage-independent growth, thus, if a chemical compound is able to inhibit this property, it will successfully transform the cancer cells to the normal cells [36]. Herein, we visualized a significant (p < 0.01) reduction in terms of colony formation in the MDA-MB-231 treated cells with compound **8j** compared to the control cells, demonstrating efficacy of compound **8j**

to kill cancer cells.

Apoptosis plays a decisive role in cancer development and is supposed to be a mechanism against cancer progression by eliminating the mutated neoplastic cells [37,38]. Thiazolidinone derivatives exert the apoptotic effect through activating PPARγ [13]. Furthermore, nitrofuran derivatives have a checked history as the anti-proliferative agents with ability to inhibit topoisomerase II [39]. On the other side, after an un-repairable DNA damage as a result of topoisomerase inhibition, cells undergo apoptosis [40]. In light of these considerations, we decided to find out whether the cytotoxic effect of compound **8j** was related to apoptosis induction by employing caspase-3 activity along with annexin/PI and DAPI staining assays. Annexin binding test is an assay in which early detection of apoptosis would be possible before loss of membrane integrity [41] and subsequently distinguishes the apoptotic from necrotic cells. Our annexin/PI findings apparently demonstrated that a significant percentage of MDA-MB-231 cells underwent apoptosis process following treatment with compound **8j** in a concentration-dependent manner; however, the higher concentration (8 μM) was excluded for further evaluation due to the presence of a large population of necrotic cells. On the other hand, one of the hallmark signs of apoptotic mode of cell death is nuclear fragmentation [42]. Hence, fluorescent DNA-binding agent (DAPI) was applied to visualize the cellular morphological changes associated with apoptosis. We found out the condensed nucleus and fragmented apoptotic bodies upon treatment with compound **8j** at 4 μM concentration indicating the apoptotic potential of compound **8j**.

As a part of our study to evaluate the role of compound **8j** in activating the process of apoptosis, we carried out Western blotting to detect cleaved caspase-3. Caspase-3 is one the members of the cysteine protease family and considered as a vital mediator to execute the programmed cell death apoptosis [43]. The activated caspase-3 proteolytically degrades the PARP, which in turns inactivates its DNA-repairing abilities during apoptosis [1,44]. Keeping in mind that MDA-MB-231 cells exhibited apoptotic bodies following treatment with compound **8j**, we next decided to determine the cleavage of caspase-3 for further confirmation. Our results clearly revealed a reduced level of procaspase-3 expression corroborating an apoptotic activity of compound **8j** at 4 μM concentration after 48 h of incubation. Combined, the above results suggest an apoptosis induction mechanism for anticancer activity of the tested compound.

Moreover, a potentially strategy to control tumor growth is modulating the cell cycle progression in cancer [45]. On the other hand, apoptosis is triggered by arresting in cell cycle [46], thus, we were encouraged to evaluate the cell cycle profile upon compound **8j** treatment. Our findings indicated that compound **8j** was able to induce cell cycle arrest at G1/S phase in a concentration-dependent manner at 48 h in MDA-MB-231 cells. These results along with accumulation of the cells in G0/G1 phase after treating with this compound, validated the apoptotic effect of compound **8j**.

In terms of breast cancer, anti-metastatic activity of thiazolidinone derivatives has been reported in MDA-MB-231 cells [23]; however, the effect of compound **8j** as a novel synthesized thazolidinone on MDA-MB-231 cells invasion remained uninvestigated. Indeed, this study attempted to uncover the anti-metastatic role of this compound on breast cancer by performing matrigel assay on MDA-MD-231 cell line as a suitable model of metastatic breast cancer. One approach for anti-metastatic therapy is disturbing the one or more steps involved in cancer metastasis including cell adhesion and invasion [47]. In metastasis process, tumor cells first traverse through the basal membrane and then enter the bloodstream; however, invasion via the basal membrane is a vital step [48,49]. Therefore, we evaluated anti-invasive property of compound **8j** using a transwell membrane system. Our outcomes showed that the number of MDA-MB-231 invaded cells significantly decreased following compound **8j** treatment at 4 μM concentration compared to the untreated cells corroborating the ability of this compound to successfully inhibit the cells penetrating the basal membrane.

On the other hand, increased expression and activity of proteolytic enzymes including MMPs are associated with the tumor cells metastasis [50]. It was reported that high expression level of MMP-9 in breast cancer contributes to high rate of lymph node metastasis, distant metastasis and poorer relapse- free survival [51–54]. Thus, we investigated the influence of compound **8j** on MMP-9 mRNA expression as our subsequent study. Our findings demonstrated that the level of MMP-9 mRNA expression in the compound **8j**-treated cells was lower than that in the control cells. The obtained data were in line with the findings of matrigel assay and suggest a further anti-metastatic role for compound **8j**, which seems not to be farfetched due to the presence of thiazolidinone and nitro furan moieties together that augmented the anti-metastatic potential of this compound, even more than that of single moiety alone [39].

In vivo animal model investigation was used to verify the reliability of the *in vitro* results to address the various issues related to anti-breast cancer properties. In our *in vivo* study, the anti-tumor and anti-metastatic effects of compound **8j** were evaluated in the 4T1 tumor-bearing mouse model that mimics initiation and progression of human triple negative breast cancer in an immune competent condition [55–57]. We found that daily i.p. administration of compound **8j** at doses of 1 and 10 mg/kg for 4 weeks (20 days) could remarkably suppress the growth of breast cancer tumor. It is of note that no considerable difference was detected on the body weight between the control and treated groups implying no obvious toxicity of the compound to the animals. As our results showed, treatment with compound **8j** at dose of 10 mg/kg/day displayed a potent tumor growth inhibition. Noteworthy is mentioning that a significant drop in tumor volume was visualized upon treatment with 1 and 10 mg/kg of compound **8j** in the second week of treatment demonstrating a rapid onset of action with a good penetration into the tumor. However, increase in the tumor volume followed a slight trend in the treated groups within the second and third weeks. Further validation by H&E staining displayed that after compound **8j** administration at 10 mg/kg, large areas of tumor cell death were visualized compared with the vehicle-control group. Moreover, tumor sections were stained for the proliferation marker, Ki-67 to verify the anti-tumor effect of compound **8j**. As expected, tumor from the treated group at 10 mg/kg demonstrated less proliferative activity. Accumulating evidence shows that microvessel density (MVD) is an essential prognostic biomarker correlates with tumor growth and development [58,59]. In other words, increased expression of CD31 and VEGF in tumor sections is connected with angiogenesis [60]. Evidently, by increasing angiogenesis, adequate blood and nutrients are provided for tumor growth and metastasis. In this study, we noted that CD31 expression was diminished in the compound **8j**-treated mice (10 mg/kg) compared with the untreated ones, which was accompanied by the H&E results.

Since metastasis is a major challenge in cancer treatment [61] and given that 4T1 cells are highly invasive and thereby primary tumor metastasizes to the lungs after establishment for 3 weeks in BALB/c mice [55,62], herein, we also focused on anti-metastatic potential of compound **8j** in our metastatic mouse model of breast cancer. In line with our transwell assay that revealed a strong inhibition of cell invasion following compound **8j** treatment, histopathological assay was carried out on the lung sections obtained from the treated and non-treated mice. Results exhibited a lower number of pulmonary nodules in the compound **8j**-treated mice at 10 mg/kg. In addition, IHC findings of the lungs demonstrated the inhibition of Ki-67 and CD31 expressions, which corroborates our *in vitro* results suggesting an anti-metastatic role for compound **8j**. Interestingly, the IHC outcomes associating with CD31 marker verified our *in vitro* results related to the MMP-9 mRNA expression. Given that MMP-9 contributes to regulating tumor angiogenesis through VEGF release from ECM store [63,64], we suggest an anti-angiogenic role for compound **8j** through inhibition of MMP-9 expression. However, further experiments will be required to unravel in greater detail the underlying mechanism.

4. Conclusions

Development of novel synthetic analogues possessing thiazolidinone structure with anticancer properties, are topics of growing interest in medicinal chemistry. In the current study, compound **8j** as a new thiazolidinone derivative exhibited a promising anticancer and anti -metastatic activity in the *in vitro* and *in vivo* models of TNBC. The potential effect of compound **8j** is most likely through induction of apoptosis with G1/S arrest and inhibition of angiogenesis as well. These findings are owed not only to the thiazolidinone scaffold but also to the nitrofuran moiety.

5. Experimental

5.1. Chemicals

Chemicals were purchased from Merck and Sigma/Aldrich Companies. Melting points were taken on an electrothermal IA 9300 capillary melting-point apparatus (Ontario, Canada) and are uncorrected. 1H NMR spectra were obtained using a Bruker FT-400 or FT-500 spectrometers (Bruker, Rheinstetten, Germany). Mass spectra were obtained using a 5973 Network Mass Selective Detector at 70 eV (Agilent technology). FT-IR spectra were recorded using a Shimadzu FT-IR 8400S spectrographs (KBr disks). Elemental analysis was carried out with a Perkin-Elmer Model 240-c apparatus (Perkin Elmer, Norwalk, CT, USA) at Faculty of Science, University of Tehran. The results of the elemental analyses (C, H, N) were within ± 0.4% of the calculated amounts.

5.2. General procedures for the synthesis of compounds *8a-8k*

In a Dean-Starck trap, the hydrazide **(7)** 0.8 mmol and corresponding aromatic aldehydes 0.8 mmol were refluxed in toluene about 3 h. After the end of the reaction, thioglycolic acid 2.4 mmol was added and the mixture was refluxed 24–48 h. Finally, following checking the reaction by TLC, toluene was evaporated and the remaining was neutralized by $NaHCO_3$ 10% solution. The resulting precipitate was purified by crysallization in ethanol or 1,4-Dioxan to give the target compounds **8a-8k** [65,66].

N-(4-oxo-2-phenylthiazolidin-3-yl)-2-(phenylthio)benzamide (8a). Yield 70%; m.p = 231–232 °C (1,4-Dioxan); IR (KBr): υ cm^{-1} 3155(NH), 1695(C═O), 1670(C═O).^{1}H NMR (500 MHz,$CDCl_3$): δ ppm 8.02 (s,1H,NH), 7.57 (d, *J* = 7.6 Hz,1H, aromatic, H_6), 7.45–7.43 (m, 2H, aromatic, $H_{2'}$,$H_{6'}$), 7.34–7.32 (m, 3H, aromatic, H_4, $H_{3'}$, $H_{5'}$), 7.29–7.28 (m, 3H, aromatic, H_5, H_2-phenyl, H_6-phenyl), 7.26–7.25 (m, 3H, H_3,H_4, H_5-phenyl), 7.24–7.18 (t, 1H, aromatic, $H_{4'}$), 7.07 (d, *J* = 8.0 Hz, 1H, aromatic, H_3), 6.10 (s,1H, Ar-CH), 3.87 (d, *J* = 15.9 Hz, S-CH), 3.71 (d, *J* = 15.9 Hz, S-CH). ^{13}C NMR (126 MHz, DMSO-d_6): *δ* 170.02, 166.20, 137.22, 136.78, 133.88, 132.80, 132.53, 131.95, 131.64, 129.77, 129.65, 129.27, 129.16, 128.31, 128.24, 126.69, 62.92, 30.25. MS: *m/z* (%) 406 (M^+, 3), 230 (2.3), 213 (100), 184(62), 152 (7), 93 (95), 77 (13), 51 (9). Anal. Calcd. for $C_{22}H_{18}N_2O_2S_2$: C, 65.00; H, 4.46; N, 6.89. Found: C, 65.31; H, 4.78; N, 6.58.

N-(2-(4-fluorophenyl)-4-oxothiazolidin-3-yl)-2-(phenylthio) benzamide (8b). Yield 98%; m.p = 218–219 °C (4-Dioxan); IR(KBr): νcm^{-1} 3159(NH), 1710(C═O), 1668(C═O).^{1}H NMR (500 MHz, DMSO-d_6): *δ* 10.72 (s, 1H, NH), 7.56–7.52 (m, 2H, aromatic, H_4, H_6), 7.39 (bs, 3H, aromatic, H_5, $H_{2'}$, $H_{6'}$), 7.37–7.30 (m, 4H, aromatic, $H_{3'}$, $H_{5'}$, H_2-fluorophenyl, H_6- fluorophenyl), 7.25 (t, *J* = 7.3 Hz, 1H, aromatic, $H_{4'}$), 7.17 (t, *J* = 8.5 Hz, 2H, H_3-fluorophenyl, H_5- fluorophenyl), 6.96 (d, *J* = 7.8 Hz, 1H, aromatic, H_3), 5.98 (s, 1H, Ar-CH), 3.95 (d, *J* = 16.0 Hz, 1H, S-CH), 3.83 (d, *J* = 15.9 Hz, 1H, S-CH). ^{13}C NMR (126 MHz, DMSO-d_6): *δ* 168.76, 165.93, 163.35, 161.41, 136.41, 134.27, 133.61, 132.99, 131.27, 130.32, 130.26, 129.96, 129.66, 128.31, 128.17, 126.07, 115.43, 115.26, 60.91, 29.31. MS: *m/z* (%) 424 (M+, 6), 2229 (8), 213 (100), 184 (43), 139 (10), 93 (66), 77 (5). Anal. Calcd. for $C_{22}H_{17}FN_2O_2S_2$: C, 62.25; H, 4.04; F, 4.48; N, 6.60. Found: C, 61.94; H, 4.28; N, 6.73.

N-(2-(4-chlorophenyl)-4-oxothiazolidin-3-yl)-2-(phenylthio) benzamide (8c). Yield 75%; m.p = 208–209 °C (EtOH). IR (KBr): υ cm^{-1} 3210 (NH), 1714(C═O), 1652(C═O).^{1}H NMR (500 MHz, DMSO-d_6): *δ* 10.74 (s, 1H, NH), 7.52 (d, *J* = 8.4 Hz, 2H, aromatic, H_4, H_6), 7.45–7.29 (m, 9H, H_5, $H_{2'}$, $H_{3'}$, $H_{5'}$, $H_{6'}$, H_2, H_3, H_5, H_6-chlorophenyl), 7.26 (t, *J* = 7.5 Hz, 1H, aromatic, $H_{4'}$), 6.97 (d, *J* = 7.9 Hz, 1H, aromatic, H_3), 5.97 (s, 1H, Ar-CH), 3.96 (d, *J* = 16.0 Hz, 1H, S-CH), 3.84 (d, *J* = 15.8 Hz, 1H, SCH). ^{13}C NMR (126 MHz, DMSO-d_6): *δ* 168.78, 165.95, 137.24, 136.34, 133.63, 133.55, 132.94, 131.29, 130.05, 130.00, 129.89, 129.65, 128.51, 128.31, 128.17, 126.11, 60.87, 29.27. MS: *m/z* (%) 442(M^+ +2, 1.9), 440 (M+, 5.8), 213 (100), 184 (44), 152 (9), 33 (66). Anal. Calcd. for $C_{22}H_{17}ClN_2O_2S_2$: C, 59.92; H, 3.89; N, 6.35. Found: C, 59.67; H, 4.08; N, 6.52.

N-(2-(4-bromophenyl)-4-oxothiazolidin-3-yl)-2-(phenylthio) benzamide (8d). Yield 95%; m.p = 198–199 °C (1,4-dioxan); IR (KBr): υ cm^{-1} 3122 (NH), 1695(C═O), 1664(C═O). ^{1}H NMR (500 MHz, CDCl3): *δ*(ppm) 8.08 (s, 1H, NH), 7.65 (dd, *J* = 7.5,1.3 Hz,1H, aromatic, H_6), 7.42 (d, *J* = 8.4 Hz, 2H, aromatic, $H_{2'}$, $H_{6'}$), 7.32–7.24 (m, 7H, H_4, H_5, $H_{4'}$, H_2-, H_3-, H_5-, H_6-bromophenyl), 7.19–7.17 (m, 2H, aromatic, $H_{3'}$, $H_{5'}$), 7.14 (dd, *J* = 7.91,1.1 Hz, 1H, aromatic, H_3), 5.95 (s, 1H, Ar-CH), 3.96 (d, *J* = 16.0 Hz, 1H, S-CH), 3.80 (d,*J* = 16.0 Hz, 1H, S-CH). ^{13}C NMR (75 MHz, CDCl3): *δ* 169.62, 166.01, 136.11, 135.46, 133.87, 132.84, 132.38, 132.20, 131.75, 129.85, 129.43, 127.95, 127.09, 123.74, 62.17, 30.05. MS: *m/z*(%) 486(M^+ +2,1.7), 484 (M^+, 1.6), 213 (100), 184 (73), 152 (13), 93 (96), 77 (8), 51 (7). Anal. Calcd. for $C_{22}H_{17}BrN_2O_2S_2$: C, 54.44; H, 3.53; N, 5.77. Found: C, 54.15; H, 4.08; N, 5.44.

N-(2-(4-nitrophenyl)-4-oxothiazolidin-3-yl)-2-(phenylthio)benzamide (8e). Yield 70%; m.p = 195–196 °C (EtOH); IR (KBr):υ cm^{-1} 3143(NH), 1691(C═O), 1673(C═O),1537, 1348(NO_2). ^{1}H NMR (500 MHz, DMSO-d_6): *δ* 10.99 (bs, 1H, 1H, NH), 8.15 (d, *J* = 8.2 Hz, 2H, H_3, H_5-nitrophenyl), 7.76 (d, *J* = 8.3 Hz, 2H, H_2-, H_6-nitrophenyl), 7.49–7.15 (m, 8H, H_4, H_5, H_6, $H_{2'}$, $H_{3'}$, $H_{4'}$, $H_{5'}$, $H_{6'}$), 6.99 (d, *J* = 7.9 Hz, 1H, aromatic, H_3), 6.14 (s, 1H, Ar-CH), 4.01 (d, *J* = 15.9 Hz, 1H, S-CH), 3.87 (d, *J* = 15.9 Hz, 1H, S-CH). ^{13}C NMR (126 MHz, DMSO-d_6): *δ* 168.71, 166.10, 147.59, 146.04, 133.93, 132.42, 131.23, 130.47, 129.49, 129.28, 129.14, 128.09, 128.01, 127.58, 126.35, 123.61, 60.48, 29.24. MS: *m/z* (%) 451 (M^+ +6), 213 (100), 184 (95), 152 (19), 93 (60), 77(13), 57(14), 51 (9). Anal. Calcd. for $C_{22}H_{17}N_3O_4S_2$: C, 58.52; H, 3.80; N, 9.31. Found: C, 58.89; H, 3.47; N, 8.93.

N-(4-oxo-2-(pyridin-2-yl)thiazolidin-3-yl)-2-(phenylthio)benzamide (8f). Yield 95%; m.p = 203–204 °C (1,4-Dioxan); IR (KBr):υ cm^{-1} 3184(NH), 1712(C═O), 1679(C═O). ^{1}H NMR (500 MHz,$CDCl_3$): *δ*(ppm) 8.59 (bs, 1H, NH), 8.55 (d, *J* = 4.7 Hz,1H, H_6-pyridyl), 7.70–7.65 (m, 2H, aromatic, H_6-, H_4-pyridyl), 7.34 (d, *J* = 7.4 Hz, 1H, H_3-pyridyl), 7.31–7.20 (m, 8H, aromatic, H_4, H_5, $H_{2'}$, $H_{3'}$, $H_{4'}$, $H_{5'}$, $H_{6'}$, H_5-pyridyl), 7.07 (d, *J* = 7.6 Hz, 1H, aromatic, H_3), 6.17 (s, 1H, Ar-CH), 3.86 (d, *J* = 15.8 Hz, 1H, S-CH), 3.71 (d, *J* = 15.8 Hz, 2H, S-CH). ^{13}C NMR (126 MHz, CDCl3): *δ* 170.43, 166.23, 157.51, 150.06, 137.43, 134.13, 134.11, 133.20, 132.38, 131.84, 131.77, 129.57, 129.43, 128.05, 126.86, 123.83, 122.35, 62.71, 29.53. MS: *m/z*(%) 408 (M^+ +1, 13), 407(M^+, 6), 229 (9), 213(100), 184(51), 179 (38), 152 (9), 93(45), 77 (60, 51 (10). Anal. Calcd. for $C_{21}H_{17}N_3O_2S_2$: C, 61.90; H, 4.21; N, 10.31. Found: C, 62.12; H, 4.10; N, 10.02.

N-(4-oxo-2-(pyridin-3-yl)thiazolidin-3-yl)-2-(phenylthio)benzamide (8g). Yield 90%; m.p = 168–169 °C (1,4-Dioxan). IR (KBr): υ cm^{-1} 3161 (NH), 1714 (C═O), 1674 (C═O). ^{1}H NMR (500 MHz, $CDCl_3$): *δ*(ppm) 9.52(s, 1H, NH), 8.81 (s, 1H, H_2-pyridyl), 8.51(dd, *J* = 5.1,1.3 Hz, 1H, H_6-pyridyl), 8.02 (d, *J* = 7.7 Hz, 1H, H_4-pyridyl), 7.61 (d, *J* = 7.6 Hz, 1H, aromatic, H_6), 7.37–7.36 (m, 1H, aromatic, H_4), 7.29–7.22 (m, 6H, aromatic, H2′, H3′, H4′, H5′, H6′, H_5-pyridyl), 7.21–7.15 (t, *J* = 7.5 Hz, 1H, aromatic, H_5), 7.01(d, *J* = 7.8 Hz, 1H,

aromatic, H_3), 6.19 (s, 1H, Ar-CH), 3.86 (d, J = 12.6 Hz, 1H, S-CH), 3.75 (d, J = 12.6 Hz, 1H, S-CH). ^{13}C NMR (75 MHz, CDCl3): δ 169.44, 156.70, 149.72, 149.10, 137.22, 136.62, 133.94, 133.74, 132.63, 132.54, 131.65, 131.04, 129.50, 128.76, 128.07, 126.39, 123.82, 60.43, 30.11. MS: *m/z*(%) 407 (M^+, 5), 230 (2), 213 (100), 184 (95), 152(18), 93 (36), 77 (7), 51 (8), 46 (9). Anal. Calcd. for $C_{21}H_{17}N_3O_2S_2$: C, 61.90; H, 4.21; N, 10.31. Found: C, 61.64; H, 4.25; N, 10.14.

N-(2-(furan-2-yl)-4-oxothiazolidin-3-yl)-2-(phenylthio)benzamide (8h). Yield 65%; m.p = 178–180 °C (1,4-Dioxan). IR (KBr): υ cm^{-1} 3148(NH), 1701(C═O), 1682(C═O). ^{1}H NMR (500 MHz, DMSO-d_6): δ 10.87 (bs, 1H, NH), 7.73 (bs, 1H, aromatic, H_6), 7.42 (bs, 5H, aromatic, $H_{2'}$, $H_{3'}$, $H_{5'}$, $H_{6'}$, H_5-furyl), 7.36 (t, J = 7.7 Hz, 1H, aromatic, H_4), 7.26 (t, J = 7.5 Hz, 1H, aromatic, H_5), 6.97 (d, J = 8.0 Hz, 1H, aromatic, H_3), 6.59 (s, 1H, H_4-furyl), 6.44 (s, 1H, H_3-furyl), 6.01 (s, 1H, Ar-CH), 3.89 (d, J = 16.0 Hz, 1H, S-CH), 3.79 (d, J = 15.9 Hz, 1H, S-CH). ^{13}C NMR (126 MHz, DMSO-d_6): δ 168.19, 166.01, 149.94, 144.22, 136.95, 133.27, 133.35, 133.01, 132.90, 131.35, 129.74, 129.65, 128.44, 125.89, 110.67, 110.42, 54.56, 28.86. MS: *m/z* (%) 397 (M^+ +1, 8), 396 (M^+, 11), 229 323 (4.5), 229 (14), 213 (100), 184(38), 152(8), 93(81), 77 (4.8), 51 (8.5), 46 (12). Anal. Calcd. for $C_{20}H_{16}N_2O_3S_2$: C, 60.59; H, 4.07; N, 7.07. Found: C, 60.48; H, 3.79; N, 6.83.

N-(4-oxo-2-(thiophen-2-yl)thiazolidin-3-yl)-2-(phenylthio)benzamide (8i). Yield 60%; m.p = 180–182 °C (1,4-Dioxan). IR (KBr): υ cm^{-1} 3158 (NH), 1713 (C═O), 1673 (C═O). ^{1}H NMR (500 MHz, DMSO-d_6): δ 10.82 (s, 1H, NH), 7.65 (d, J = 4.9 Hz, 1H, aromatic, H_6), 7.41 (bs, 5H, aromatic, $H_{2'}$, $H_{3'}$, $H_{5'}$, $H_{6'}$, H_4), 7.39–7.34 (m, 2H, aromatic, H_5, H_5-thienyl), 7.25 (d, J = 8.8 Hz, 2H, aromatic, H_3, $H_{4'}$), 6.97 (t, J = 7.0 Hz, 2H, H_3, H_4-thienyl), 6.26 (s, 1H, Ar-CH), 3.91 (d, J = 16.4 Hz, 1H, S-CH), 3.86 (d, J = 16.1 Hz, 1H, S-CH). ^{13}C NMR (126 MHz, DMSO-d_6): δ 168.25, 166.01, 142.81, 141.71, 133.17, 132.63, 131.33, 130.88, 129.74, 129.69, 129.12, 128.99, 128.39, 128.27, 126.76, 125.92, 57.07, 29.41. MS: *m/z*(%) 412 (M^+,3), 229(16), 213(100), 184 (69), 152 (13), 93(96), 77 (6), 51 (7). Anal. Calcd. $C_{20}H_{16}N_2O_2S_3$: C, 58.23; H, 3.91; N, 6.79. Found: C, 57.91; H, 3.77; N, 6.68.

N-(2-(5-nitrofuran-2-yl)-4-oxothiazolidin-3-yl)-2-(phenylthio) benzamide (8j). Yield 47%; m.p = 156–157 °C (1,4-Dioxan). IR(KBr): υ cm^{-1} 3158 (NH), 1713 (C═O), 1673 (C═O).^{1}H NMR (400 MHz,DMSO-d_6): δ(ppm) 10.82 (s, 1H, NH), 7.61 (bs,1H, aromatic, H_6), 7.49 (d, J = 7.2 Hz,1H, H_4-furyl), 7.38–6.99 (m,9H,Ar,furan), 6.09 (s,1H,Ar-CH), 3.97–3.81(2d, J = 16.0 Hz, 2H, S-CH_2). ^{1}H NMR (500 MHz, DMSO-d_6): δ 10.87 (s, 1H, NH), 7.64 (bs, 1H, H_4-furyl), 7.49 (d, J = 6.5 Hz, 1H, aromatic, H6), 7.42–7.30 (m, 6H, aromatic, H_4, H_5, $H_{2'}$, $H_{3'}$, $H_{5'}$, $H_{6'}$), 7.09–7.01 (m, 3H, aromatic, H_3, $H_{4'}$, H_3-nitrofuryl), 6.10 (s, 1H, Ar-CH), 3.98 (d, J = 15.9 Hz, 1H, S-CH), 3.85 (d, J = 15.9 Hz, 1H, s-CH). ^{13}C NMR (126 MHz, DMSO-d_6): δ 168.04, 166.02, 154.50, 151.59, 136.61, 135.57, 132.99, 132.76, 131.49, 131.27, 129.96, 129.70, 128.33, 126.14, 113.87, 113.63, 54.35, 28.69. MS: *m/z*(%) 441 (M^+, 6), 213(100), 184 (50), 152(9), 93 (22), 77 (5), 69 (3), 51 (10). Anal. Calcd. $C_{20}H_{15}N_3O_5S_2$: C, 54.41; H, 3.42; N, 9.52. Found: C, 54.57; H, 3.29; N, 9.73.

N-(2-(5-nitrothiophen-2-yl)-4-oxothiazolidin-3-yl)-2-(phenylthio)benzamide (8k). Yield 50%, m.p = 185–186 °C (1,4-Dioxan); IR (KBr): υ cm^{-1} 3157 (NH), 1710 (C═O), 1668 (C═O), 1510, 1348 (NO_2). ^{1}H NMR (500 MHz, DMSO-d_6): δ 10.91 (s, 1H, NH), 7.95 (d, J = 4.4 Hz, 1H, H_4-nitrothienyl), 7.48 (d, J = 7.6 Hz, 1H, aromatic, H_6), 741–7.34 (m, 7H, H_4, H_5, $H_{2'}$, $H_{3'}$, $H_{5'}$, $H_{6'}$, H_3-nitrothienyl), 7.31 (t, J = 7.5 Hz, 1H, aromatic, $H_{4'}$), 7.01 (d, J = 8.0 Hz, 1H, aromatic, H_3), 6.27 (s, 1H, Ar-CH), 4.03 (d, J = 16.0 Hz, 1H, S-CH), 3.88 (d, J = 16.1 Hz, 1H, S-CH). ^{13}C NMR (126 MHz, DMSO-d_6): δ 168.04, 166.08, 151.64, 151.13, 136.22, 133.74, 133.44,132.68, 131.47, 130.30, 129.65, 129.49, 128.49, 128.28, 128.21, 126.32, 56.88, 29.07. MS: *m/z*(%) 457 (M^+, 6), 213 (100), 184 (47), 152(8),93 (32), 77 (5), 69 (6), 51(6.5), 46 (9). Anal. Calcd. $C_{20}H_{15}N_3O_4S_3$ C, 52.50; H, 3.30; N, 9.18. Found: C, 52.23; H, 3.53; N, 8.98.

5.3. Cell culture

Adenocarcinoma breast cancer (MDA-MB-231, C578), human colon carcinoma (HT-29, C466), human hepatocyte carcinoma (HepG2, C158), mouse mammary tumor (4T1, C604) and human gingival fibroblast (HGF-1, C165) cell lines were obtained from National Cell Bank of Pasteur Institute of Iran (NCBI). Cells were grown in Dulbecco's Minimum Essential Medium (DMEM) (Gibco-BRL, Rockville, IN) containing 10% (v/v) Fetal Bovine Serum (FBS), 2 mM L-glutamine, 100 units/ml penicillin G, and 100 μg/ml streptomycin (Gibco-BRL, Rockville, IN). Then, cells were maintained in a humidifier atmosphere of 5% CO_2 at 37 °C.

5.4. Cell cytotoxicity assay

In this test, MTT (3-(4,5dimethylthiazol-2-yl)-2,5-diphenyl tetrazolium bromide) is reduced to the insoluble purple-blue formazan crystals precipitated by the living cells [67]. Briefly, chemical compounds were solubilized in DMSO (Dimethyl Sulfoxide) and then diluted with medium to the desired concentrations (0.1–50 μM), whereas DMSO final concentration was maintained at < 0.5%. Cell cytotoxicity assay was carried out in two stages: a preliminary screening at a unique concentration (10 μM) of compounds at 72 h **(8a-8k)** and an IC_{50} determination test with the increasing concentrations for the selected compounds with the percentage of cytotoxicity more than 60% at 24, 48 and 72 h. Tested cells were plated in 96-well plates at a density of 1–5 × 10^3 cells/well for (MDA-MB-231), 3–7 × 10^3 cells/well for (HT-29 and HepG2) and 5 × 10^3 for HGF-1 in the proper culture medium. Twenty-four hours following seeding, cells were exposed to the interesting compounds for 24, 48 and 72 h. After completion of the incubation time, 20 μl of MTT dye solution (5 mg/ml in PBS) was added to each well and the plates were further incubated at 37 °C for 4 h. The visible formazan crystals formed by mitochondrial succinate dehydrogenase in the live cells, were then solubilized in DMSO and the optical density was quantified at 570 nm by using an ELISA plate reader (Epoch2, Biotek, USA). Relative cell cytotoxicity was calculated compared to the non-treated cells.

5.5. Annexin V/PI assay

Apoptosis was tracked by an Annexin V/PI kit obtained from Roche Applied Science (Indianapolis, IN, USA) according to the manufacturer's instructions with minor modification [68]. This experiment was performed to quantify the percentage of live, apoptotic and necrotic cells upon compounds treatment. MDA-MB-231 cells were seeded at a density of 5 × 10^4 cells/well and exposed to 2, 4 and 8 μM concentrations of compound **8j** for 48 h. Following washing the cells with PBS, cells were gently re-suspended in 100 μl of binding buffer. Afterwards, annexin V-FLUOS (0.5 μl) and PI (0.5 μl) solutions were added and then the tubes were incubated for 10 min in the dark before being analyzed by flow cytometry.

5.6. Cell cycle distribution analysis

The effect of compound **8j** on cell cycle progression was assessed by a standard Propidium Iodide (PI) staining procedure followed by flow cytometry analysis [67]. MDA-MB-231 cells were exposed to 2 and 4 μM concentrations of compound **8j** for 48 h. The cells were then gathered and fixed using 70% ice-cold ethanol at −20 °C for 24 h. Following treating the cells with RNase A (20 mg/ml) and PI (1 mg/ml) for 15 min at 37 °C, the samples were analyzed with PARTEC flow cytometer (PARTEC GmbH, Munster, Germany) using FlowJo software. Cell populations were distributed into three subsets of cells representing G0/G1, S and G2/M phases.

5.7. DAPI staining

Cell nuclear morphology was investigated by using fluorescence microscopy upon DAPI staining. MDA-MB-231 cells were seeded in 24-well plates and treated with 2 and 4 μM concentrations of compound **8j** for 48 h. After staining the cells with a DAPI solution (2.5 μg/ml) for 15 min at 37 °C, the cells were washed with PBS and methanol and the nuclear changes were observed by a fluorescence microscope (Nikon eclipse TS100) [69].

5.8. Transwell invasion assay

The Transwell assay was conducted to explore the cell invasion capability [70]. In the current study, invasion assay was performed with the 24-well Transwell culture chamber with 8 μm pores (SPL Life Sciences, Korea) coated with sixty microliters of diluted matrigel (0.5 mg/ml, BD Biosciences, San Jose, USA) on the inner surface. Untreated and treated MDA-MB-231 cells with 4 μM concentration of compound **8j** for 48 h, were then starved and suspended in 200 μl of serum-free medium and implanted into the upper section of the Transwell culture chamber. Afterwards, 750 μl of the culture medium supplemented with 10% FBS was added to the lower compartment in order to attract cells. Upon incubating at 37 °C for 24 h, non-invaded cells were removed from the top of the matrigel using a cotton-tipped swab and the cells on the underside of the membrane were washed and fixed in 4% PFA and stained for 20 min in crystal violet solution (0.5 mg/ml). Finally, four random fields of the penetrated cells in each well were counted by using a microscope at 10X magnification in order to assess the invasiveness.

5.9. Soft agar colony formation assay

For this experiment, treated cells with 4 μM concentration of compound **8j** for 48 h were seeded in 6-well plates at a density of 5000 cells/well. Following suspending the cells in DMEM containing 0.35% low-melting agarose, the cells were plated onto solidified 0.5% agarose having DMEM in 6-well culture plates and allowed to grow for 22 days in 5% CO2 at 37 °C. After washing and air-drying the cells, the colonies were manually counted in five fields [71]. Phase contrast micrographs of the colonies were taken with a Nikon microscope (Nikon, Tokyo, Japan).

5.10. Western blotting

MDA-MB-231 cells (5×10^4 per well) were seeded in 6-well plates and treated with 2 and 4 μM concentrations of compound **8j** for 48 h. Total protein was extracted using ice-cold lysis buffer consisting of Tris 62.5 mM (pH 6.8), DTT 50 mM, SDS 10%, glycerol and the protease inhibitor [69]. The protein concentration was determined by Bradford assay [72]. Almost 40 μg of protein was loaded onto the 15% sodium dodecyl sulfate polyacrylamide gel electrophoresis (SDS-PAGE), separated electrophoretically and transferred onto the PVDF membrane (GE Health Care Life Sciences, Buckinghamshire, UK). Membranes were then blocked in 1% (w/v) casein for overnight and probed with antibodies targeting caspase-3 (Abcam, ab13847, Cambridge, UK) at 1:500 dilution. After washing, the membranes were incubated with the secondary antibody conjugated with horseradish peroxidase (Cell Signaling Technology, 7074S, Beverly, MA) at 1:8000 dilution for two hours at room temperature. GAPDH (Glyceraldehyde phosphate dehydrogenase) (Abcam, ab37168, Cambridge, UK) was used to confirm equal loading in wells. Following washing steps, the blots were visualized with the ECL (Enhanced Chemiluminescence) advance Western blotting detection kit obtained from GE Healthcare Life Sciences (Buckinghamshire, UK) to compare the amount of proteins in each lane. The black values were determined using Image J software.

5.11. Determination of MMP-9 mRNA level

mRNA expression of MMP-9 (Matrix Metalloproteinase-9) was assessed by quantitative real-time polymerase chain reaction (qRT-PCR) [73]. To do it, Trizol (Invitrogen, USA) was applied to extract total RNA from the cells. Then, RNA was reverse-transcribed using the Superscript First-Strand Synthesis System (ThermoFisher Scientific, USA). Primers for MMP-9 and GAPDH as a housekeeping gene were designed by AlleleID6 software (PREMIER Biosoft International, USA). All primers were checked against the GenBank database to ensure that no similarities remained with other known human DNA sequences

5.12. In vivo study

Thirty two female BALB/c mice (5–7 weeks, 18–20 g weights) were obtained from the National Animal Center (Pasteur Institute of Karaj) and maintained under standard conditions of 12/12-h light–dark cycle, with food and water provided *ad libitum*. Animals were treated in accordance with the guidelines approved by the animal ethics committee of Tehran Medical Sciences, Islamic Azad University (IR.IAU.PS.REC.1398.104). Mice were subcutaneously implanted with 10^6 cells/50 μl of exponentially 4T1 cells at the mammary fat pad [15].Then the mice bearing tumor were randomly assigned into four groups (n = 8). Ten days after cancer cell inoculation, treatments were initiated five days a week and lasted for 4 weeks. To explore the antitumor effect of compound **8j**, mice were intra-peritoneally injected by vehicle alone (DMSO) and two doses of the compound (1 and 10 mg/kg/day) for 20 days. Mice received no treatment in the negative control group. Following measuring the tumor volumes in two dimensions thrice a week by a digital caliper during the treatment period, they were calculated according to the formula: (length × width^2)/2. Daily monitoring of the mice was conducted by the same observer to check toxicity including weight loss, discomfort and death. The animals were anesthetized with 60 mg/kg of sodium pentobarbital and then chest was surgically opened and concurrently perfused by 0.9% saline. Following removing the tumors and lungs from the animals, samples were placed in 10% formalin for fixation and histopathological analysis.

5.13. Histology and immunohistochemistry

Mice were euthanized and then after tissues were perfused, harvested and fixed in 10% neutral buffered formalin solution. The tissues were subsequently embedded in paraffin, sectioned longitudinally at 5 μm and stained with hematoxylin and eosin (H&E). For immunohistochemistry, the tissue sections were prepared in the same manner as those used for H&E staining [71]. In addition, tissue sections were assessed for angiogenesis and proliferation using common markers, CD31 (Abcam, ab28364, Cambridge, UK, 1:50 dilution), and Ki-67 (Abcam, ab15580, Cambridge, UK, 1:200 dilution). Briefly, upon de-paraffinization and antigen retrieving the sections by boiling in 10 mM sodium citrate for 30 min, the slides were incubated with the primary antibodies diluted in blocking buffer and kept at 4°C overnight. Then, the sections were washed with PBS and incubated with biotinylated secondary antibody using an HRP/DAB (Horseradish peroxidase/3,3'-diaminobenzidine) detection IHC kit (Abcam, ab64264, Cambridge, UK) according to the manufacturer's instructions and finally analyzed by an expert pathologist. Images were taken using a Carl Zeiss AxioImager microscope and Image M1 Software (Carl Zeiss, Jena, Germany) (magnification, 200 and 400×). The percentage of positive tumor cells within 5 high-randomly fields were accounted for IHC expression level of Ki-67. For microvessel density, brown-stained vessels were counted in the selected fields.

5.14. Statistical analysis

All data were analyzed using the Graph Pad Prism 6.0 Software. For all the measurements, unpaired *t-test* and one-way ANOVA followed by

Tukey's post-hoc test was used to assess the statistical significance between groups. $p \leq 0.05$ was considered to be statistically significant.

Declaration of competing interest

The authors declare that they have no known competing financial interests or personal relationships that could have appeared to influence the work reported in this paper.

Acknowledgments

We acknowledge Dr. Ahad Mohammadnejad of the Department of Cancer Biology, Research Center, Cancer Institute of Iran, Tehran University of Medical Sciences for excellent technical support. This research was financially supported by the Iran National Science Foundation grant No 96010968 and Pasteur Institute of Iran for providing materials and research facilities to prepare this valuable document.

Ethics approval

All animals used in the study were handled in accordance with the guidelines approved by the animal ethics committee of Tehran Medical Sciences, Islamic Azad University.

Appendix A. Supplementary material

Supplementary data to this article can be found online at https://doi.org/10.1016/j.bioorg.2020.104276.

References

[1] B.G. Utage, M.S. Patole, P.V. Nagvenkar, S.S. Kamble, R.N. Gacche, Prosopis juliflora (Sw.), DC induces apoptosis and cell cycle arrest in triple negative breast cancer cells: in vitro and in vivo investigations, Oncotarget 9 (2018) 33050, https://doi.org/10.18632/oncotarget.26095.

[2] K.W. Luo, G.G.L. Yue, C.H. Ko, J.K.M. Lee, S. Gao, L.F. Li, G. Li, K.P. Fung, P.C. Leung, S.L. Clara Bik, In vivo and in vitro anti-tumor and anti-metastasis effects of Coriolus versicolor aqueous extract on mouse mammary 4T1 carcinoma, Phytomedicine 21 (2014) 1078–1087, https://doi.org/10.1016/j.phymed.2014.04.020.

[3] L.Y. Jia, M.K. Shanmugam, G. Sethi, A. Bishayee, Potential role of targeted therapies in the treatment of triple-negative breast cancer, Anticancer Drugs 27 (2016) 147–155, https://doi.org/10.1097/CAD.0000000000000328.

[4] C. Wang, S. Kar, X. Lai, W. Cai, F. Arfuso, G. Sethi, P.E. Lobie, B.C. Goh, L.H. Lim, M.J. Hartman, Triple negative breast cancer in Asia: an insider's view, Cancer Treat. Rev. 62 (2018) 29–38, https://doi.org/10.1016/j.ctrv.2017.10.014.

[5] R.H. Alvarez, V. Valero, G.N. Hortobagyi, Emerging targeted therapies for breast cancer, J. Clin. Oncol. 28 (2010) 3366–3379, https://doi.org/10.1200/JCO.2009.25.4011.

[6] E.A. Perez, J.P. Spano, Current and emerging targeted therapies for metastatic breast cancer, Cancer 118 (2012) 3014–3025, https://doi.org/10.1002/cncr.26356.

[7] Y. Oikawa, E. Matsuda, T. Nishii, Y. Ishida, M.J. Kawaichi, Down-regulation of CIBZ, a novel substrate of caspase-3, induces apoptosis, J. Biol. Chem. 283 (2008) 14242–14247, https://doi.org/10.1074/jbc.M802257200.

[8] R.S. Wong, Apoptosis in cancer: from pathogenesis to treatment, J. Exp. Clin. Cancer Res. 30 (2011) 87, https://doi.org/10.1186/1756-9966-30-87.

[9] C. Park, H.J. Shin, G.Y. Kim, T.K. Kwon, T.J. Nam, S.K. Kim, J. Cheong, I.W. Choi, Y.H. Choi, Induction of apoptosis by streptochlorin isolated from Streptomyces sp. in human leukemic U937 cells, Toxicol. Vitro. 22 (2008) 1573–1581, https://doi.org/10.1016/j.tiv.2008.06.010.

[10] R.W. Johnstone, A.A. Ruefli, S.W. Lowe, Apoptosis: a link between cancer genetics and chemotherapy, Cell 108 (2002) 153–164, https://doi.org/10.1016/s0092-8674(02)00625-6.

[11] A. Verma, S.K. Saraf, 4-Thiazolidinone–A biologically active scaffold, Eur. J. Med. Chem. 43 (2008) 897–905, https://doi.org/10.1016/j.ejmech.2007.07.017.

[12] J. Lu, K. Imamura, S. Nomura, K.I. Mafune, A. Nakajima, T. Kadowaki, N. Kubota, Y. Terauchi, G. Ishii, A. Ochiai, Chemopreventive effect of peroxisome proliferator–activated receptor γ on gastric carcinogenesis in mice, Cancer Res. 65 (2005) 4769–4774, https://doi.org/10.1158/0008-5472.

[13] C. Blanquicett, J. Roman, C.M. Hart, Thiazolidinediones as anti-cancer agents cancer research, Cancer Ther. 6 (2008) 25–34.

[14] A.C. Tripathi, S.J. Gupta, G.N. Fatima, P.K. Sonar, A. Verma, S.K. Saraf, 4-Thiazolidinones: the advances continue…, Eur. J. Med. Chem. 72 (2014) 52–77, https://doi.org/10.1016/j.ejmech.2013.11.017.

[15] E. Mousavi, S. Tavakolfar, A. Almasirad, Z. Kooshafar, S. Dehghani, A. Afsharinasab, A. Amanzadeh, S. Shafiee, M. Salimi, In vitro and in vivo assessments of two novel hydrazide compounds against breast cancer as well as mammary tumor cells, Cancer Chemother. 79 (2017) 1195–1203, https://doi.org/10.1007/s00280-017-3318-5.

[16] S. Tavakolfar, E. Mousavi, A. Almasirad, A. Amanzadeh, S.M. Atyabi, P. Yaghamii, S. Samiee-Sadr, M. Salimi, In vitro anticancer effects of two new potent hydrazide compounds on leukemic cells, Anti-Cancer Agents Med. Chem. 16 (2016) 1646–1651, https://doi.org/10.2174/1871520616666160404112945.

[17] A. Deep, B. Narasimhan, S.M. Lim, K. Ramasamy, R.K. Mishra, V. Mani, 4-Thiazolidinone derivatives: synthesis, antimicrobial, anticancer evaluation and QSAR studies, RSC Adv. 6 (2016) 109485–109494, https://doi.org/10.1039/C6RA23006G.

[18] A. Almasirad, A. Shafiee, M. Abdollahi, A. Noeparast, N. Shahrokhinejad, N. Vousooghi, S.A. Tabatabai, R. Khorasani, Synthesis and analgesic activity of new 1, 3, 4-oxadiazoles and 1, 2, 4-triazoles, Med. Chem. Res. 20 (2011) 435–442, https://doi.org/10.1007/s00044-010-9335-0.

[19] A. Almasirad, S. Samiee-Sadr, A. Shafiee, Synthesis and antimycobacterial activity of 2-(Phenylthio) benzoylarylhydrazone derivatives, Iran J. Pharm. Res. 10 (2011) 727–731.

[20] A. Almasirad, N. Vousooghi, S.A. Tabatabai, A. Kebriaeezadeh, A. Shafiee, Synthesis, anticonvulsant and muscle relaxant activities of substituted 1, 3, 4-oxadiazole, 1, 3, 4-thiadiazole and 1, 2, 4-triazole, Acta Chim. Slov. 54 (2007) 317–324.

[21] J.A. Hickman, Apoptosis induced by anticancer drugs, Cancer Metastasis Rev. 11 (1992) 121–139, https://doi.org/10.1007/BF00048059.

[22] N.N. Danial, S.J. Korsmeyer, Cell death: critical control points, Cell 116 (2004) 205–219, https://doi.org/10.1016/s0092-8674(04)00046-7.

[23] J. Zuo, Y. Yu, M. Zhu, W. Jing, M. Yu, H. Chai, C. Liang, J. Tu, Inhibition of miR-155, a therapeutic target for breast cancer, prevented in cancer stem cell formation, Cancer Biomark. 21 (2018) 383–392, https://doi.org/10.3233/CBM-170642.

[24] K. Kessenbrock, V. Plaks, Z. Werb, Matrix metalloproteinases: regulators of the tumor microenvironment, Cell 141 (2010) 52–67, https://doi.org/10.1016/j.cell.2010.03.015.

[25] L. Herszényi, I. Hritz, G. Lakatos, M. Varga, Z. Tulassay, The behavior of matrix metalloproteinases and their inhibitors in colorectal cancer, Int. J. Mol. Sci. 13 (2012) 13240–13263, https://doi.org/10.3390/ijms131013240.

[26] L.J. Van't Veer, H. Dai, M.J. Van De Vijver, Y.D. He, A.A. Hart, M. Mao, H.L. Peterse, K. Van Der Kooy, M.J. Marton, A.T. Witteveen, Gene expression profiling predicts clinical outcome of breast cancer, Nature 415 (2002) 530–536, https://doi.org/10.1038/415530a.

[27] L. Tang, X. Ma, Q. Tian, Y. Cheng, H. Yao, Z. Liu, X. Qu, X. Han, Inhibition of angiogenesis and invasion by DMBT is mediated by down regulation of VEGF and MMP-9 through Akt pathway in MDA-MB-231 breast cancer cells, Food Chem. Toxicol. 56 (2013) 204–213, https://doi.org/10.1016/j.fct.2013.02.032.

[28] F. Bray, J.S. Ren, E. Masuyer, J.J. Ferlay, Global estimates of cancer prevalence for 27 sites in the adult population in 2008, Int. J. Cancer. 132 (2013) 1133–1145, https://doi.org/10.1002/ijc.27711.

[29] M. Bingul, O. Tan, C. Gardner, S. Sutton, G. Arndt, G. Marshall, B. Cheung, N. Kumar, D. Black, Synthesis, characterization and anti-cancer activity of hydrazide derivatives incorporating a quinoline moiety, Molecules 21 (2016) 916, https://doi.org/10.3390/molecules21070916.

[30] J. Rudolph, Cdc25 phosphatases: structure, specificity, and mechanism, Biochemistry 46 (2007) 3595–3604, https://doi.org/10.1021/bi700026j.

[31] W. Wang, Nitrofuran derivatives that induce apoptosis in breast cancer cells by activating protein expression, U.S. Patent Application 15/735,700, 2018.

[32] J.K. Andrade, M.I. Souza, M.A. Gomes Filho, D.M. Silva, A.L. Barros, M.D. Rodrigues, P.B. Silva, S.C. Nascimento, J.S. Aguiar, D.J. Brondani, N-pentyl-nitrofurantoin induces apoptosis in HL-60 leukemia cell line by upregulating BAX and downregulating BCL-xL gene expression, Pharmacol. Rep. 68 (2016) 1046–1053, https://doi.org/10.1016/j.pharep.2016.06.004.

[33] C.H. Tseng, C.C. Tzeng, C.C. Chiu, C.Y. Hsu, C.K. Chou, Y.L. Chen, Discovery of 2-[2-(5-nitrofuran-2-yl) vinyl] quinoline derivatives as a novel type of anti metastatic agents, Bioorg. Med. Chem. 23 (2015) 141–148, https://doi.org/10.1016/j.bmc.2014.11.015.

[34] H. Duan, Y. Li, H.Y. Lim, W. Wang, Identification of 5-nitrofuran-2-amide derivatives that induce apoptosis in triple negative breast cancer cells by activating C/EBP-homologous protein expression, Bioorg. Med. Chem. 23 (2015) 4514–4521, https://doi.org/10.1016/j.bmc.2015.06.011.

[35] C. Thieury, N. Lebouvier, R. Le Guével, Y. Barguil, G. Herbette, C. Antheaume, E. Hnawia, Y. Asakawa, M. Nour, T. Guillaudeux, Mechanisms of action and structure-activity relationships of cytotoxic flavokawain derivatives, Bioorg. Med. Chem. 25 (2017) 1817–1829, https://doi.org/10.1016/j.bmc.2017.01.049.

[36] Y. Zhao, M. Turlington, D.J. LaPar, D.R. Jones, D.A. Harris, I.L. Kron, L. Pu, C.L. Lau, Characterization of novel synthesized small molecular compounds against non-small cell lung cancer, Ann. Thorac. Surg. 92 (2011) 1031–1037, https://doi.org/10.1016/j.athoracsur.2011.04.081.

[37] S. Elmore, Apoptosis: a review of programmed cell death, Toxicol. Pathol. 35 (2007) 495–516, https://doi.org/10.1080/01926230701320337.

[38] F.H. Igney, P.H. Krammer, Death and anti-death: tumour resistance to apoptosis, Nat. Rev. Cancer 2 (2002) 277–288, https://doi.org/10.1038/nrc776.

[39] M. Polycarpou-Schwarz, K. Müller, S. Denger, A. Riddell, J. Lewis, F. Gannon, G. Reid, Thanatop: a novel 5-nitrofuran that is a highly active, cell-permeable inhibitor of topoisomerase II, Cancer Res. 67 (2007) 4451–4458, https://doi.org/10.1158/0008-5472.CAN-07-0393.

[40] A. Monger, N. Boonmuen, K. Suksen, R. Saeeng, T. Kasemsuk, P. Piyachaturawat, W. Saengsawang, A. Chairoungdua, Inhibition of topoisomerase IIα and induction of apoptosis in gastric cancer cells by 19-triisopropyl andrographolide, Asian Pac. J. Cancer Prev. 18 (2017) 2845–2851, https://doi.org/10.22034/APJCP.2017.18.10.2845.
[41] A.M. Alabsi, R. Ali, A.M. Ali, S.A.R. Al-Dubai, H. Harun, N.H. Abu Kasim, A. Alsalahi, Apoptosis induction, cell cycle arrest and in vitro anticancer activity of gonothalamin in a cancer cell lines, Asian Pac. J. Cancer Prev. 13 (2012) 5131–5136, https://doi.org/10.7314/apjcp.2012.13.10.5131.
[42] S. Kasibhatla, G.P. Amarante-Mendes, D. Finucane, T. Brunner, E. Bossy-Wetzel, D.R. Green, Acridine orange/ethidium bromide (AO/EB) staining to detect apoptosis, CSH Protoc. (2006), https://doi.org/10.1101/pdb.prot4493.
[43] Y.E. Liu, C.C. Tong, Y.B. Zhang, P.F. Cong, X.Y. Shi, Y. Liu, L. Shi, Z. Tong, H.X. Jin, M.X. Hou, Chitosan oligosaccharide ameliorates acute lung injury induced by blast injury through the DDAH1/ADMA pathway, PLoS ONE 13 (2018) (2018) e0192135, https://doi.org/10.1371/journal.pone.0192135. eCollection.
[44] I. Kitazumi, M. Tsukahara, Regulation of DNA fragmentation: the role of caspases and phosphorylation, FEBS J. 278 (2011) 427–441, https://doi.org/10.1111/j.1742-4658.2010.07975.x.
[45] X. Graña, E.P. Reddy, Cell cycle control in mammalian cells: role of cyclins, cyclin dependent kinases (CDKs), growth suppressor genes and cyclin-dependent kinase inhibitors (CKIs), Oncogene 11 (1995) 211–219.
[46] S. Pajaniradje, K. Mohankumar, R. Pamidimukkala, S. Subramanian, R. Rajagopalan, Antiproliferative and apoptotic effects of Sesbania grandiflora leaves in human cancer cells, Biomed Res. Int. 2014 (2014) 474953, https://doi.org/10.1155/2014/474953.
[47] H.S. Lee, E.Y. Seo, N.E. Kang, W.K. Kim, [6]-Gingerol inhibits metastasis of MDA-MB-231 human breast cancer cells, J. Nut. Biochem. 19 (2008) 313–319, https://doi.org/10.1016/j.jnutbio.2007.05.008.
[48] W.G. Stetler-Stevenson, S. Aznavoorian, L.A. Liotta, Tumor cell interactions with the extracellular matrix during invasion and metastasis, Annu. Rev. Cell Biol. 9 (1993) 541–573, https://doi.org/10.1146/annurev.cb.09.110193.002545.
[49] A.E. Yu, R.E. Hewitt, D.E. Kleiner, W.G. Stetler-Stevenson, Molecular regulation of cellular invasion—role of gelatinase A and TIMP-2, Biochem. Cell Biol. 74 (1996) 823–831, https://doi.org/10.1139/o96-088.
[50] L. Ning, H. Ma, Z. Jiang, L. Chen, L. Li, Q. Chen, H. Qi, Curcumol suppresses breast cancer cell metastasis by inhibiting MMP-9 via JNK1/2 and Akt-dependent NF-κB signaling pathways, Integr. Cancer Ther. 15 (2016) 216–225, https://doi.org/10.1177/1534735416642865.
[51] H.C. Li, D.C. Cao, Y. Liu, Y.F. Hou, J. Wu, J.S. Lu, G.H. Di, G. Liu, F.M. Li, Z.L. Ou, Prognostic value of matrix metalloproteinases (MMP-2 and MMP-9) in patients with lymph node-negative breast carcinoma, Breast Cancer Res. Treat. 88 (2004) 75–85, https://doi.org/10.1007/s10549-004-1200-8.
[52] F. Vizoso, L. Gonzalez, M. Corte, J. Rodriguez, J. Vazquez, M. Lamelas, S. Junquera, A. Merino, J. Garcia-Muniz, Study of matrix metalloproteinases and their inhibitors in breast cancer, Br. J. Cancer 96 (2007) 903–911, https://doi.org/10.1038/sj.bjc.6603666 Epub 2007 Mar 6.
[53] L. Hao, C. Zhang, Y. Qiu, L. Wang, Y. Luo, M. Jin, Y. Zhang, T.B. Guo, K. Matsushima, Y. Zhang, Recombination of CXCR4, VEGF, and MMP-9 predicting lymph node metastasis in human breast cancer, Cancer Lett. 253 (2007) 34–42, https://doi.org/10.1016/j.canlet.2007.01.005.
[54] Z.S. Wu, Q. Wu, J.H. Yang, H.Q. Wang, X.D. Ding, F. Yang, X.C. Xu, Prognostic significance of MMP-9 and TIMP-1 serum and tissue expression in breast cancer, Int. J. Cancer 122 (2008) 2050–2056, https://doi.org/10.1002/ijc.23337.
[55] K. Tao, M. Fang, J. Alroy, G.G. Sahagian, Imagable 4T1 model for the study of late stage breast cancer, BMC Cancer 8 (2008) 228, https://doi.org/10.1186/1471-2407-8-228.
[56] P. Ottewell, R. Coleman, I. Holen, From genetic abnormality to metastases: murine models of breast cancer and their use in the development of anticancer therapies, Breast Cancer Res. Treat. 96 (2006) 101–113, https://doi.org/10.1007/s10549-005-9067-x.
[57] V.C. Jordan, Proven value of translational research with appropriate animal models to advance breast cancer treatment and save lives: the tamoxifen tale, Br. J. Clin. Pharmacol. 79 (2015) 254–267, https://doi.org/10.1111/bcp.12440.
[58] K.C. Mei, J. Bai, S. Lorrio, J.T.W. Wang, K.T. AlJamal, Investigating the effect of tumor vascularization on magnetic targeting in vivo using retrospective design of experiment, Biomaterials 106 (2016) 276–285, https://doi.org/10.1016/j.biomaterials.2016.08.030.
[59] S.P. Robinson, J.K. Boult, N.S. Vasudev, A.R. Reynolds, Monitoring the vascular response and resistance to sunitinib in renal cell carcinoma in vivo with susceptibility contrast MRI, Cancer Res. 77 (2017) 4127–4134, https://doi.org/10.1158/0008-5472.CAN-17-0248.
[60] H. Li, G. Tan, X. Jiang, H. Qiao, S. Pan, H. Jiang, J.R. Kanwar, X.J. Sun, Therapeutic effects of matrine on primary and metastatic breast cancer, Am. J. Chin. Med. 38 (2010) 1115–1130, https://doi.org/10.1142/S0192415X10008512.
[61] J. O'Shaughnessy, Extending survival with chemotherapy in metastatic breast cancer, Oncologist 10 (2005) 20–29, https://doi.org/10.1634/theoncologist.10-90003-20.
[62] C.J. Aslakson, F.R. Miller, Selective events in the metastatic process defined by analysis of the sequential dissemination of subpopulations of a mouse mammary tumor, Cancer Res. 52 (1992) 1399–1405.
[63] G. Bergers, R. Brekken, G. McMahon, T.H. Vu, T. Itoh, K. Tamaki, K. Tanzawa, P. Thorpe, S. Itohara, Z. Werb, Matrix metalloproteinase-9 triggers the angiogenic switch during carcinogenesis, Nature Cell Biol. 2 (2000) 737–744, https://doi.org/10.1038/35036374.
[64] J.C. Rodríguez-Manzaneque, T.F. Lane, M.A. Ortega, R.O. Hynes, J. Lawler, M.L. Iruela-Arispe, Thrombospondin-1 suppresses spontaneous tumor growth and inhibits activation of matrix metalloproteinase-9 and mobilization of vascular endothelial growth factor, PNAS 98 (2001) 12485–12490, https://doi.org/10.1073/pnas.171460498.
[65] M. Faizi, R. Jahani, S.A. Ebadi, S.A. Tabatabai, E. Rezaee, M. Lotfaliei, M. Amini, A. Almasirad, Novel 4-thiazolidinone derivatives as agonists of benzodiazepine receptors: design, synthesis and pharmacological evaluation, EXCLI J. 16 (2017) 52–62, https://doi.org/10.17179/excli2016-692.
[66] A. Kunzler, P.D. Neuenfeldt, A.M. das Neves, C.M. Pereira, G.H. Marques, P.S. Nascente, M.H. Fernandes, S.O. Huebner, W. Cunico, Synthesis, antifungal and cytotoxic activities of 2-aryl-3-((piperidin-1-yl) ethyl) thiazolidinones, Eur. J. Med. Chem. 64 (2013) 74–80, https://doi.org/10.1016/j.ejmech.2013.03.030.
[67] F. Farmani, M. Moein, A. Amanzadeh, H.M. Kandelous, Z. Ehsanpour, M. Salimi, Antiproliferative evaluation and apoptosis induction in MCF-7 cells by Ziziphus spina christi leaf extracts, Asian Pac. J. Cancer Prev. 17 (2016) 315–321, https://doi.org/10.7314/apjcp.2016.17.1.315.
[68] M. Norouzi, S. Norouzi, M. Amini, A. Amanzadeh, S. Irian, M. Salimi, Apoptotic effects of two COX-2 inhibitors on breast adenocarcinoma cells through COX-2 independent pathway, J. Cell. Biochem. 116 (2015) 81–90, https://doi.org/10.1002/jcb.24944.
[69] S. Norouzi, M. Norouzi, M. Amini, A. Amanzadeh, M. Nabiuni, S. Irian, M. Salimi, Two COX-2 inhibitors induce apoptosis in human erythroleukemia K562cells by modulating NF-κB and FHC pathways, DARU J. Pharmaceutic. Sci. 24 (2016) 1, https://doi.org/10.1186/s40199-015-0139-0.
[70] K. Moradi, F. Barneh, S. Irian, M. Amini, R. Moradpoor, A. Amanzadeh, S. Choopani, H. Rahimi, T. Ghodselahi, M. Salimi, Two novel tri-aryl derivatives attenuate the invasion-promoting effects of stromal mesenchymal stem cells on breast cancer, Anticancer Agents Med. Chem. 19 (2019) 1002–1011, https://doi.org/10.2174/1871520619666190212123912.
[71] S. Dehghani, Z. Kooshafar, A. Almasirad, R. Tahmasvand, F. Moayer, A. Muhammadnejad, S. Shafiee, M. Salimi, A novel hydrazide compound exerts anti-metastatic effect against breast cancer, Biol. Res. 52 (2019) 40, https://doi.org/10.1186/s40659-019-0247-2.
[72] O. Ernst, T. Zor, Linearization of the bradford protein assay, J. Vis. Exp. 38 (2010) 1918, https://doi.org/10.3791/1918.
[73] W.J. Piotrowski, P. Górski, T. Pietras, W. Fendler, J. Szemraj, The selected genetic polymorphisms of metalloproteinases MMP2, 7, 9 and MMP inhibitor TIMP2 in sarcoidosis, Med. Sci. Monit. 17 (2011) CR598-607, https://doi.org/10.12659/MSM.881987.